AD NUMBER

AD813365

LIMITATION CHANGES

TO:

Approved for public release; distribution is unlimited.

FROM:

**Distribution authorized to U.S. Gov't. agencies and their contractors;
Administrative/Operational Use; 26 JAN 1967.
Other requests shall be referred to Air Force Applications Center, Washington, DC 20333.**

AUTHORITY

AFTAC USAF ltr 25 Jan 1972

SCIENCE SERVICES DIVISION

TEXAS INSTRUMENTS INCORPORATED

AFTAC Project VT/4053

P-WAVE SIGNAL EXTRACTION USING 3-COMPONENT SUBSYSTEMS AT TFO

ARRAY RESEARCH SPECIAL REPORT NO. 21

Prepared by

William Johnson and James Bonner

Program Manager

George Burrell

TEXAS INSTRUMENTS INCORPORATED
Science Services Division
P.O. Box 5621
Dallas, Texas 75222

Prepared for

AIR FORCE TECHNICAL APPLICATIONS CENTER
VELA SEISMOLOGICAL CENTER
Washington, D.C. 20333

Contract No. AF 33(657)-12747
ARPA Order No. 104-60
Project Code No. 8100

26 January 1967

ABSTRACT

Results of an initial analysis of long-period and short-period data collected at the Tonto Forest Seismological Observatory (TFO) are presented in this report. The objective of this work is experimental evaluation of the 3-component systems' capability to reject noise by exploiting the relationship between horizontal and vertical components of the seismic noise field.

Short-period data analyzed included three 8-min recordings consisting of two teleseismic signals and one noise sample, while long-period data included one 40-min teleseismic signal (encompassing the P through L interval) and one 40-min noise sample. The long-period data was taken from the 200-km dia extended array with 50-km minimum element spacing, while the short-period data was taken from the 10-km TFO cross-array.

Long-period P- and S-waves appeared extremely reproducible across the array, indicating minimal vertical crustal filtering variations. Horizontally traveling surface waves are disorganized by scattering within the array. Over the usable frequency band, the shape and magnitude of the noise spectra showed variations of ±1 db (P-wave), ±3 db (S-wave) and ±6 db (surface waves). Coherence across the array was high for the P- and S-waves and very low for the surface waves. While lacking reliable gain corrections, the short-period P-waves also appear to be well equalized (±2 db spectral variation with high coherence among elements).

Results of analyzing 3-component array processing for P-wave enhancement with the long-period instruments generally agree with the expected performance for an essentially uncorrelated noise field.

However, some coherence was found to exist between vertical and adjacent horizontal instruments around 0.12 cps, and about 3 db additional noise rejection was achieved at that point. Similar though less impressive results were obtained for the short-period 3-component processors with 2 db additional rejection achieved in the 4- to 6-sec microseism band. Thus, some noise rejection using the horizontals to predict the vertical appears to be experimentally confirmed.

TABLE OF CONTENTS

Section	Title	Page
	ABSTRACT	ii
I	INTRODUCTION	I-1
II	SUMMARY	II-1
	A. ANALYSIS PROCEDURES AND OBJECTIVES	II-1
	B. CONCLUSIONS	II-3
III	DESCRIPTION OF DATA	III-1
	A. LONG-PERIOD DATA	III-1
	B. SHORT-PERIOD DATA	III-1
IV	3-COMPONENT LONG-PERIOD DATA ANALYSIS	IV-1
	A. SIGNAL EQUALIZATION STUDIES	IV-1
	B. P-WAVE SIGNAL ENHANCEMENT PROCESSORS	IV-7
V	3-COMPONENT SHORT-PERIOD DATA ANALYSIS	V-1
	A. SIGNAL EQUALIZATION STUDIES	V-1
	B. P-WAVE SIGNAL ENHANCEMENT PROCESSORS	V-3
VI	CONCLUSIONS	VI-1
VII	REFERENCES	VII-1/2

LIST OF TABLES

Table	Title	Page
III-1	Summary of Signal and Noise Events	III-2

LIST OF ILLUSTRATIONS

Figure	Description	Page
III-1	Long-Period Noise Sample	III-3
III-2	Long-Period Signal Sample (Rat Islands)	III-4
III-3	Short-Period Noise and Signal Samples	III-6
IV-1	TFO 3-Component Long-Period Seismometer Locations	IV-2

LIST OF ILLUSTRATIONS (CONTD)

Figure	Description	Page
IV-2	Geological Summary of Extended TFO Array Locale	IV-3
IV-3	Superimposed P-Wave Power Density Spectra for Vertical Components of Rat Islands Signal	IV-5
IV-4	Superimposed S-Wave Power Density Spectra and Coherence Functions for Vertical, Radial and Transverse Components of Rat Islands Signal	IV-6
IV-5	Superimposed L-Wave Power Density Spectra and Coherence Functions for Vertical, Radial and Transverse Components of Rat Islands Signal	IV-7
IV-6	Results of Interpolating for JR Z Noise (3-Channel)	IV-10
IV-7	Results of Interpolating for SG Z Noise (3 Channel)	IV-11
IV-8	Results of Interpolating for SN Z Noise (3-Channel)	IV-12
IV-9	Results of Interpolating for WO Z Noise (3-Channel)	IV-13
IV-10	Results of Interpolating for SG Z Noise (9 Channel)	IV-14
IV-11	Predictability Functions	IV-16
IV-12	Results of Beam-Steering	IV-18
IV-13	Noise and Signal Power Ratios for Beam-Steering	IV-19
IV-14	Response of 5-Channel Signal Extraction Filter	IV-20
IV-15	Results of Applying 5-Channel MCF	IV-22
IV-16	Results of Applying 9-Channel MCF	IV-23
IV-17	Noise and Signal Power Ratios for 5-Channel MCF	IV-24
IV-18	Noise and Signal Power Ratios for 9-Channel MCF	IV-25
IV-19	Comparison of Long-Period Signal Enhancement Processors	IV-26
V-1	TFO 3-Component Short-Period Seismometer Locations	V-2
V-2	Superimposed P-Wave Power Density Spectra and Coherence for Vertical Components	V-4
V-3	Correlation Matrices for Vertical Component of Signal P-Wave	V-5

LIST OF ILLUSTRATIONS (CONTD)

Figure	Description	Page
V-4	Results of Interpolating for Z61 Noise	V-7
V-5	Results of Interpolating for Z68 Noise	V-8
V-6	Results of Interpolating for Z13 Noise	V-9
V-7	Predictability of Vertical Components	V-11
V-8	Results of Beam-Steer Processors	V-13
V-9	Noise and Signal Ratios for Beam-Steer Processors	V-14
V-10	Results of Applying 9-Channel Signal Extraction Processor	V-16
V-11	Noise and Signal Ratios for 9-Channel Signal Extraction Processors	V-17
V-12	Comparison of Short-Period Signal Enhancement Processors	V-18

SECTION I
INTRODUCTION

This special report describes a study of 3-component short-period and long-period data recorded on the extended array at the Tonto Forest Seismological Observatory (TFO) during 1965. The objective of this study is the preliminary evaluation of the effectiveness of 3-component array instrumentation in extracting teleseismic signals. Investigated areas include:

- Teleseismic signal characteristics observed both on the long-period and short-period extended crossarrays
- P-wave extraction capabilities using 3-component subsystems
- Potential contributions of 3-component array instrumentation to the event detection and classification problem

Effective monitoring of underground nuclear tests requires the ability to detect low-level teleseismic signals in the presence of seismic noise. The use of 3-component recording systems can exploit the relationship between horizontal and vertical components of the seismic noise field for additional noise rejection. The theoretical aspects of the noise-reduction capability for horizontal-vertical component combinations are described in Array Research Special Report No. 7.[1]

Using the theoretical background contained in this special report, multichannel filters for selected subsystems of seismometers are designed and applied for an experimental evaluation of P-wave extraction capability. The subsystems evaluated include:

- A single group of 3-component instruments
- A tripartite of 3-component instruments
- An array of 5 vertical component systems (long-period only)
- A 9-channel horizontal system (long-period only)

To experimentally evaluate the P-wave extraction capabilities, recordings of signals and noise were taken from the short-period and long-period 3-component instrumentation at TFO near Payson, Arizona. A large-aperture array configuration was obtained through the use of LRSM recording vans along the extended crossarray arms. The recordings were provided by AFTAC with Texas Instruments' assistance, and a TIAC* (Texas Instruments Automatic Computer) data library was formed. Array Research Special Report No. 12[2] describes the data collection and the library contents.

Statistics of the ambient noise field are of fundamental importance to the design and application of MCF systems. Accordingly, studies of the ambient noise observed on the long-period and the short-period 3-component arrays have been conducted and are described in Array Research Special Reports No. 16[3] (long-period) and No. 18[4] (short-period). Presentations of the long-period noise analysis were delivered at the VELA Seismological Center (VSC) of AFTAC on 26 July 1966.

The P-wave data must be well equalized if the P-wave extraction filters are to be effective. Therefore, a study was made of long-period and short-period teleseismic P-wave coherence and equalization. Portions of the long-period equalization study were completed previously and are presented in Array Research Special Report No. 16.[3]

*Trademark of Texas Instruments Incorporated

The following section of this report briefly summarizes the analysis procedures and findings for both the long-period and short-period data. Section III describes the data samples used for each study, and Sections IV and V contain the long-period and short-period analysis, respectively. Section VI presents the analytical conclusions and recommendations for further work.

SECTION II
SUMMARY

This section presents a summary of the TFO 3-component signal studies. It includes a brief description of analysis procedures and objectives and a discussion of resulting conclusions.

A. ANALYSIS PROCEDURES AND OBJECTIVES

The analysis program has involved studies in two areas:

- Determination of signal properties
- Evaluation of teleseismic P-wave signal-enhancement processors

Signal properties were examined to determine the extent of signal inequalization across those array instruments used in the design of the signal processors. The signal-enhancement processor evaluations sought to verify experimentally the theoretical capability for additional noise rejection resulting from exploiting the relationship between horizontal and vertical components of the seismic noise field.

Section III discusses in detail the signal and noise data used for the studies. Two well recorded signal events and a closely related noise sample were selected for the short-period analysis. The long-period studies used one signal event characterized by well recorded P-, S- and L-phases and also by a noise sample taken near in time to the signal event. The processors to be designed specified certain trace configurations which were required to be available for both signal and noise, somewhat limiting the extent of available data. These records had been previously gain-corrected at the Seismic Data Laboratory (SDL). The long-period data seems reasonably well corrected; however, the short-period gain corrections do not appear to be reliable.[5]

The P-, S- and surface phases of the long-period data were examined visually for signal reproducibility across the array. A coherence analysis was obtained for all signal phases. This analysis also yielded power-density spectra and crosscorrelations. Both were interpreted for signal similarity across the array. Similar studies were performed for the short-period P-phase arrivals, but due to the uncertain gain corrections, these studies were restricted to subjective evaluations of spectral shape similarities, correlation symmetry, etc.

Long-period signal enhancement processors which were designed and evaluated include

- Four 3-component multichannel prediction error (MPE) processors, each using the two horizontals to interpolate and remove noise on the vertical
- A beam-steer of the four MPE outputs
- A beam-steer of the four verticals used in the MPE analysis
- A 9-channel MPE using eight horizontals to interpolate and remove the noise on one vertical instrument
- A 9-channel signal extraction filter using three 3-component systems (tripartite)
- A 5-channel signal extraction filter using five verticals

All processors were designed from measured noise correlations. The extraction filters used theoretical infinite velocity signal models, and all filters were applied to the signal event and to noise samples in and adjacent to the design interval. Appropriate predictability and S/N ratio improvement curves were computed from power spectra.

Short-period signal enhancement processors include:

- Three 3-component MPE processors
- A beam-steer of the three MPE outputs
- A beam-steer of the three verticals used in the MPE analysis
- A 9-channel signal extraction filter using the three 3-component systems (tripartite)

Filter designs were similar to the long-period processors. All filters were applied to two teleseisms and to noise in and adjacent to the design interval. Evaluation proceeded on the basis of predictability and S/N ratio improvement curves.

B. CONCLUSIONS

Both the long-period and short-period equalization studies indicate that the teleseismic P-wave signals are extremely reproducible across the TFO extended array, and therefore lend themselves to array processing for signal enhancement. In addition, the long-period, S-phase energy appears to be well equalized, suggesting only minor crustal filtering variations within the array for vertically traveling energy. Similar analysis of the long-period surface wave energy suggests a more severe problem for horizontally traveling energy. Because of complex geological and topographical irregularities, it is probable that surface waves cannot traverse the array undisturbed but undergo scattering that decreases coherence.

Although the vertical and the horizontal noise fields have been found to be essentially uncorrelated at these receiver separations (except for highly directional noise sources), some correlation is found to exist at the same location between the vertical and horizontal components.

The long-period MPE and signal extraction filters demonstrate an experimental capability for using this correlation to achieve greater S/N ratio enhancement than that possible for totally uncorrelated noise. Similar, though less impressive results, were indicated for the short-period data operating on the higher-mode surface wave energy.

Analytical results indicate that 3-component preprocessing at each point within the array is feasible and can contribute to array P-wave extraction capabilities by rejecting low-velocity surface wave components that may or may not be coherent across the entire array.

SECTION III
DESCRIPTION OF DATA

This section describes the data selected for use in the long-period and short-period signal extraction and signal equalization studies. Table III-1 provides a summary of pertinent information.

A. LONG-PERIOD DATA

One noise sample and one teleseismic signal were chosen for processing from a 6-event ensemble of TFO long-period 3-component data.[3] The ensemble had previously been selected to include signals with well recorded P, S and L phases, a maximum number of usable channels and closely related noise samples. Further selection required that all signal enhancement processors be designed and applied to the same signal and noise event pair. The signal event from the Rat Islands and the noise sample (NS-1) associated with this event were chosen for this study.

Both the signal and noise data were 40-min records of 4800 data points each, sampled at 500-msec intervals. Since only the low frequency portion of the data was seismically valid, each event was digitally lowpass filtered and resampled 3:1, resulting in 1600-point records at 1500-msec sample intervals (Figures III-1 and III-2).

These events had been gain corrected by the Seismic Data Laboratory (SDL), and the gain-corrections for the vertical seismometers appear to have been performed satisfactorily. (From past array processing experience, most gain-correcting procedures using calibration data have not been successful.) However, there seems to be some difficulty with the TFO horizontals (Figures III-1 and III-2).

B. SHORT-PERIOD DATA

One noise sample (NSH-11) and two teleseismic signals (SSL-12 and SSL-30) were chosen from the TFO short-period 3-component data library.[5] The events were chosen for good seismic data on all channels

Table III-1

SUMMARY OF SIGNAL AND NOISE EVENTS

Long-Period Data

Channels Used: JR ZRT, SG ZRT, SN ZRT, WO ZRT, TFO ZRT

Noise Sample NS-1

Date: 26 September 1965 Edit Time: 055154.6 GMT

Rat Islands Signal

Date: 27 September 1965 Edit Time: 051543.0 GMT

PDE Information:

Origin Time —	050913.3	Epicentral Dist. —	53.9°
Lat. —	51.9°N	Sta.-to-Epicenter Az —	312.9°
Long. —	175.5°E	Mag. —	5.5
Depth —	41 km		

Short-Period Data

Channels Used: Z61/SE86/NE85, Z68/SE95/NE96, Z13/SE89/NE90

Noise Sample NSH-11

Date: 27 August 1965 Edit Time: 090900 GMT

Central Chilean Signal

Date: 18 August 1965 Edit Time: 101300 GMT

PDE Information:

Origin Time —	100148.1	Epicentral Dist. —	79.9°
Lat. —	37.9°S	Sta.-to-Epicenter Az —	150.7°
Long. —	73.6°W	Mag. —	4.7
Depth —	33R km		

Kermadec Islands Signal

Date: 23 August 1965 Edit Time: 214200 GMT

PDE Information:

Origin Time —	212959	Epicentral Dist. —	90.3°
Lat. —	30.8°S	Sta.to-Epicenter Az —	232.2°
Long. —	178.1°W	Mag. —	4.8
Depth —	49 km		

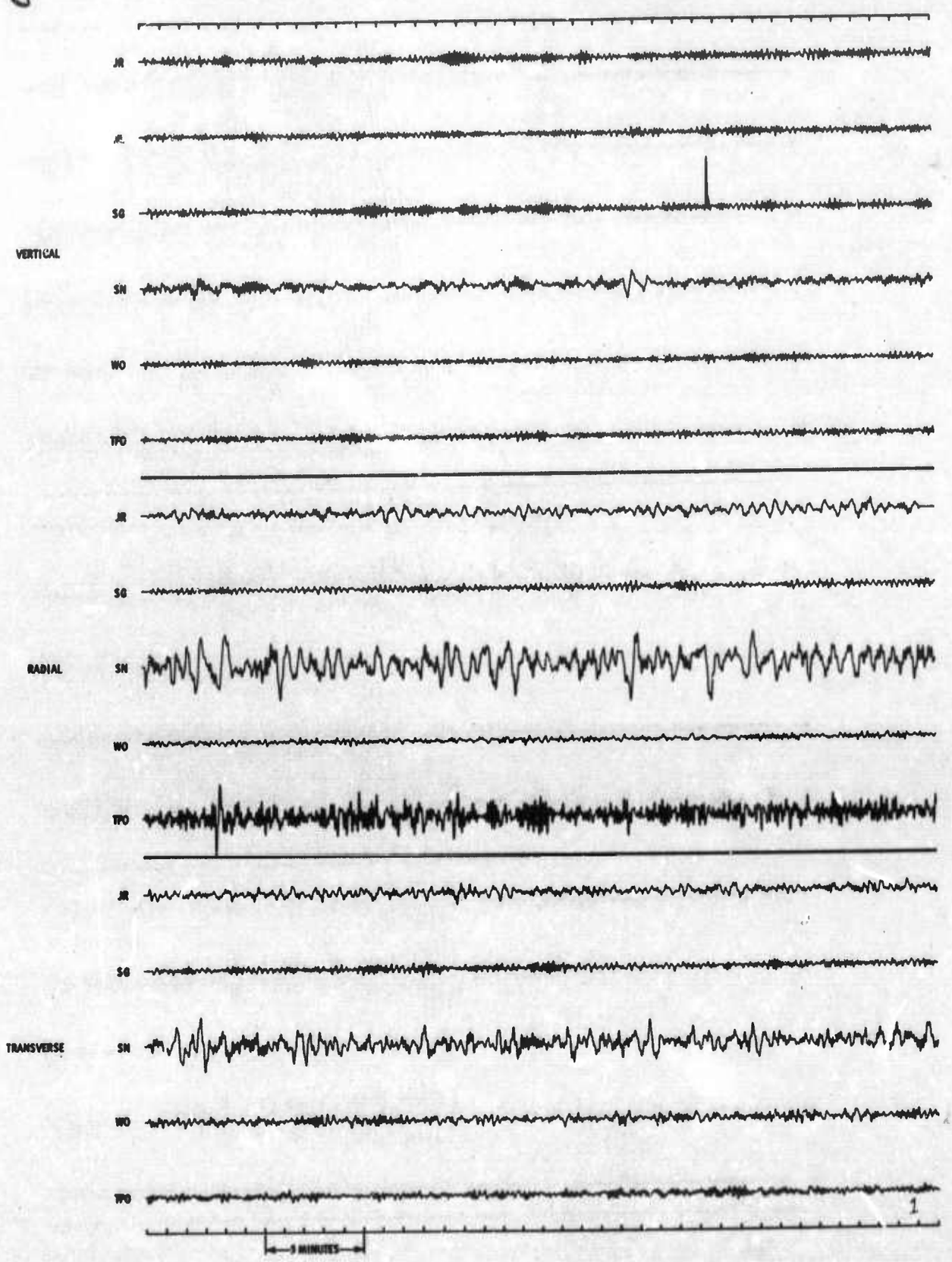

Figure III-1. Long-Period Noise Sample

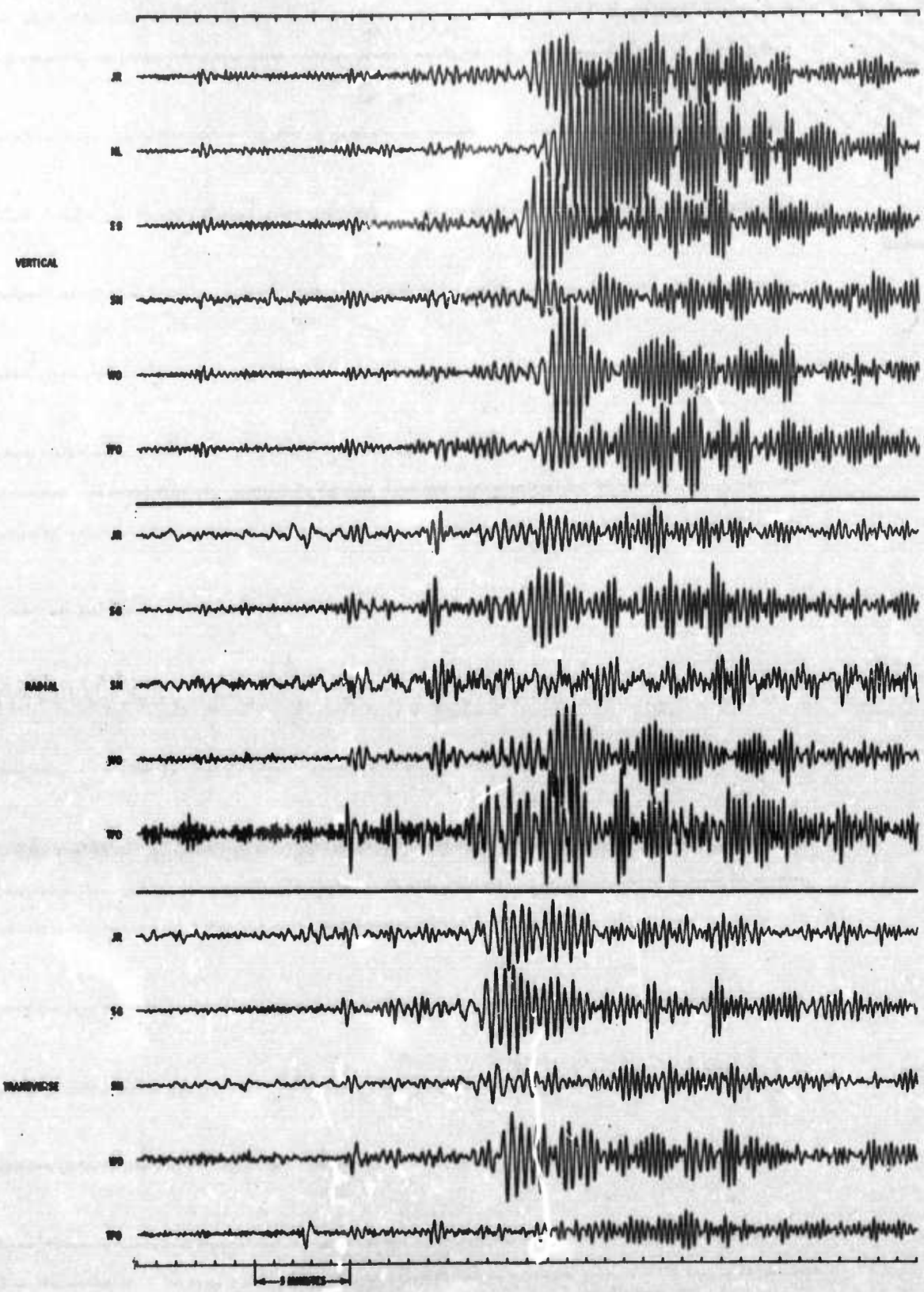

Figure III-2. Long-Period Signal Sample (Rat Islands)

of a tripartite of 3-component groups. The signals were also required to have well recorded P phases with the noise sample chosen to be reasonably close in time to the signals. The selected signal events were from Central Chile (SSL-12) and the Kermadec Islands (SSL-30) (Table III-1).

The signals and noise are each comprised of 8-min records of 9600 data points sampled at 50-msec intervals. Each event was digitally lowpass filtered and resampled 2:1, resulting in 4800-point records at 100-msec sample intervals (Figure III-3).

Gain correction of the TFO short-period data library was performed at SDL. However, due the various problems involved in the process, it has been determined that the gain corrections were not reliable.[7]

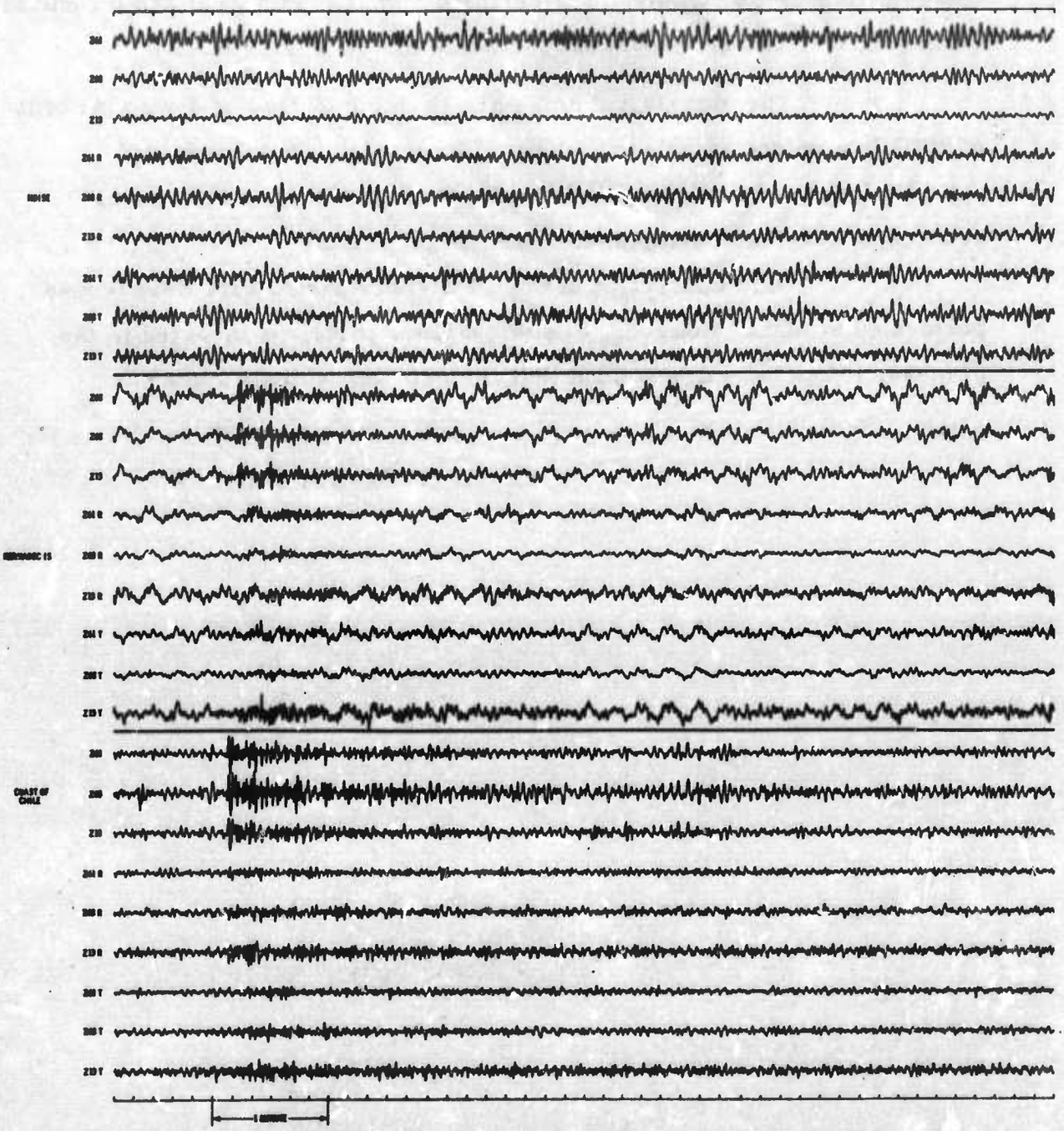

Figure III-3. Short-Period Noise and Signal Samples

SECTION IV

3-COMPONENT LONG-PERIOD DATA ANALYSIS

This section discusses in detail the signal equalization and P-wave signal enhancement studies conducted with the TFO long-period 3-component extended array. Figure IV-1 shows the location and orientation of the 3-component instruments, while Figure IV-2 illustrates the wide variations in geology over the extended array.

An investigation of the ambient noise field statistics was performed previously on a 3-component basis in the long-period frequency range.[3] Over the usable seismic bandwidth of 0.02 to 0.2 cps, the noise is essentially uncorrelated between like components due to the large receiver separations. However, in the frequency range of approximately 0.025 to 0.095 cps, the noise was found to be correlated between the vertical and horizontal components at the same location. The P-wave signal waveforms were also shown to be reproducible across the extended array.[3] Signal equalization studies were expanded to include the shear (S) and surface (L) phases.

A. SIGNAL EQUALIZATION STUDIES

Signal waveforms should be reproducible at all points within an array for effective teleseismic signal enhancement. P phase equalization has been investigated previously for one teleseismic signal.[3] Visual examination of the recorded waveforms indicated that teleseismic P-waves are highly reproducible across the array. Quantitative estimates of P-wave signal equalization through power density spectra, 2-channel coherence functions and crosscorrelation functions indicated excellent reproducibility over the frequency range of 0.04 to 0.07 cps. Power density spectra of the

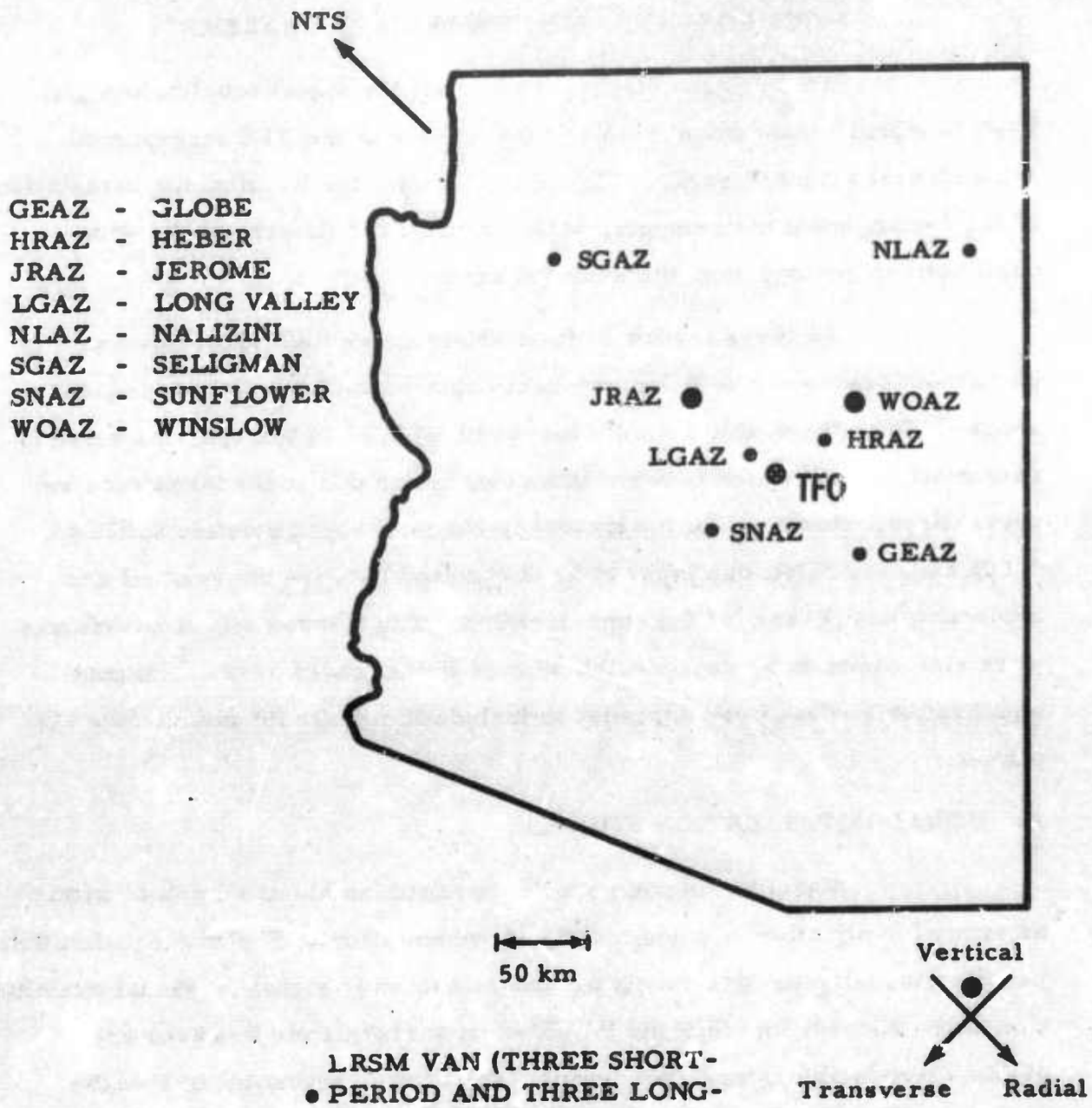

Figure IV-1. TFO 3-Component Long-Period Seismometer Locations

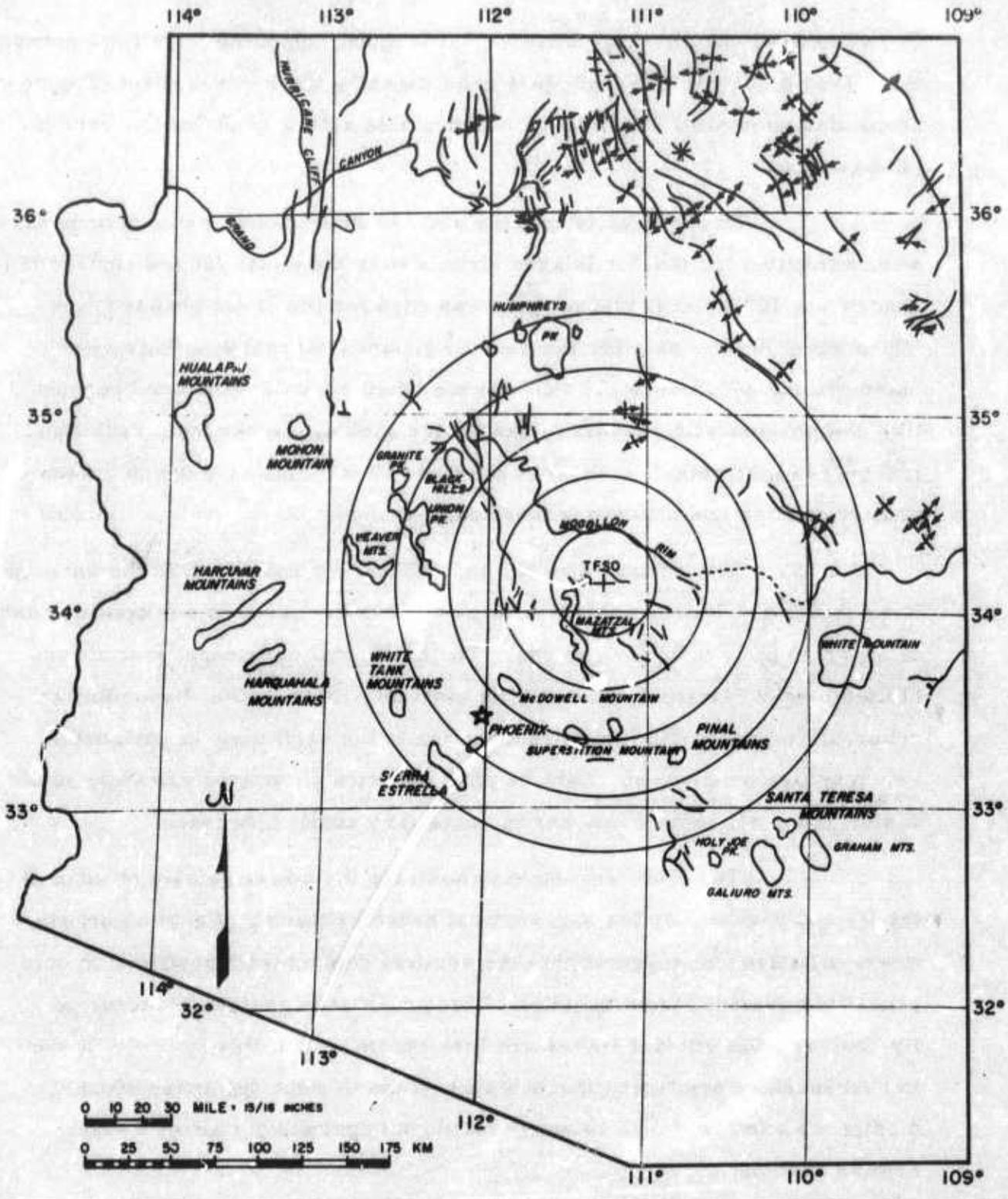

Figure IV-2. Geological Summary of Extended TFO Array Locale

P-wave signal used in this analysis (Rat Islands) computed from total correlations over a 50-point (75-sec) gate encompassing the P-wave onset (Figure IV-3) also show the P-wave to be reproducible within ±1 db for the vertical components.

Power density spectra and 2-channel coherence functions also were computed for the Rat Islands signals over the shear (S) and surface (L) phases. A 100-point (150-sec) gate was used for the shear phases and a 500-point (750-sec) gate for the surface phases. Correlation lags were computed for ±73.5 sec. The coherence functions were computed between like components with respect to van JR for each of the vertical, radial and transverse instruments. Figures IV-4 and IV-5 display the computed power density spectra and coherence functions.

Shear phase spectra and coherences indicate that the vertical components are reproducible within ±3 db over the array in a frequency band of approximately 0.02 to 0.08 cps. The horizontal component spectra exhibited larger variations than did the vertical, although they have similar coherence values. This was probably due to the variations in horizontal seismometer orientation. Surface phase spectra show approximately ±6 db variation for all components and indicate very small coherence.

The close agreement shown for the power density spectra of the P- and S-wave implies that vertical crustal filtering effects do not show much variation and suggests that the vertical component magnification compensations (derived from on-site calibrations) were reasonably accurate. By contrast, the surface waves are less reproducible; this is probably due to near-surface scattering mechanisms within or near the array which modify the surface waves severely but do not appreciably affect P- and S-wave arrivals.

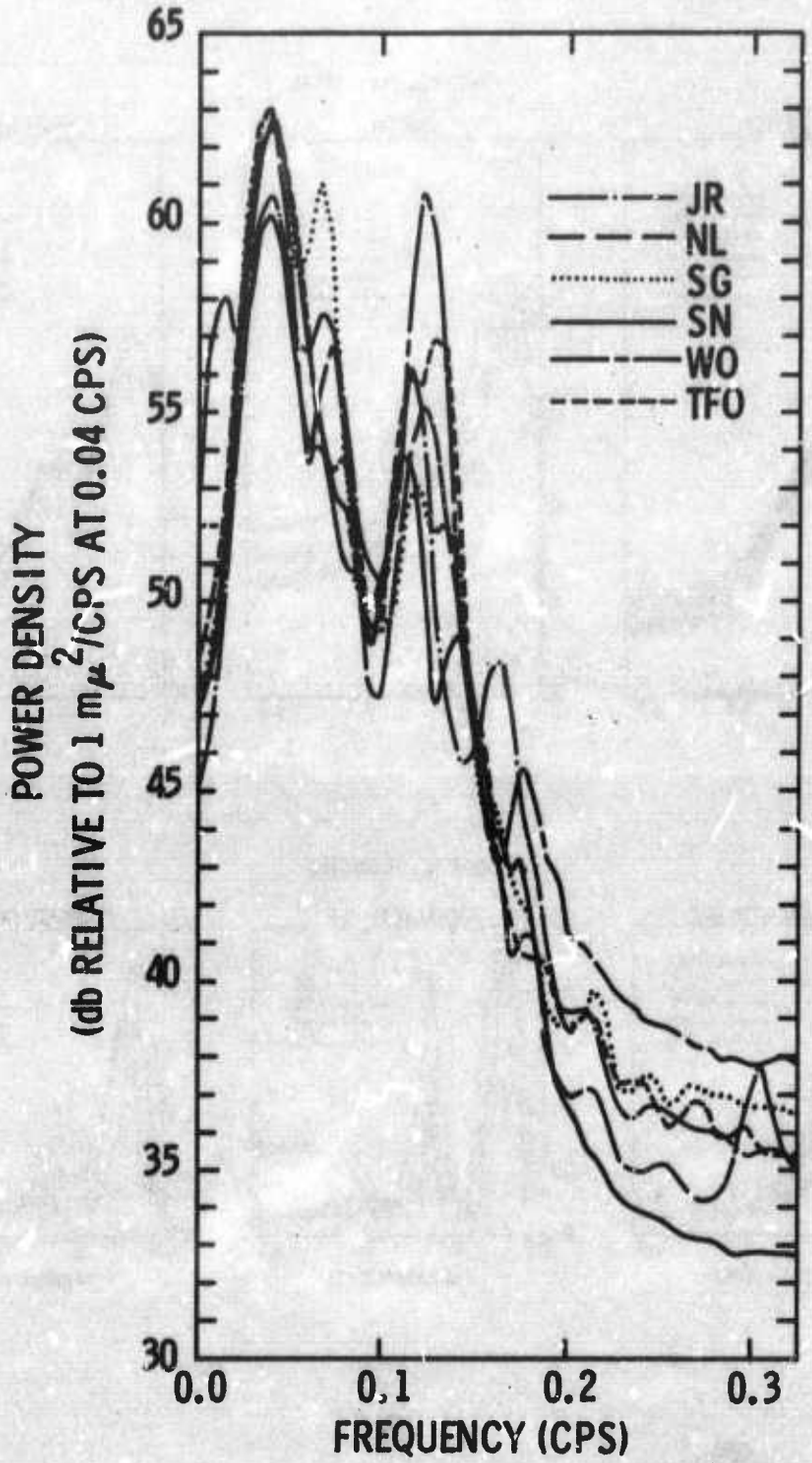

Figure IV-3. Superimposed P-Wave Power Density Spectra for Vertical Components of Rat Islands Signal

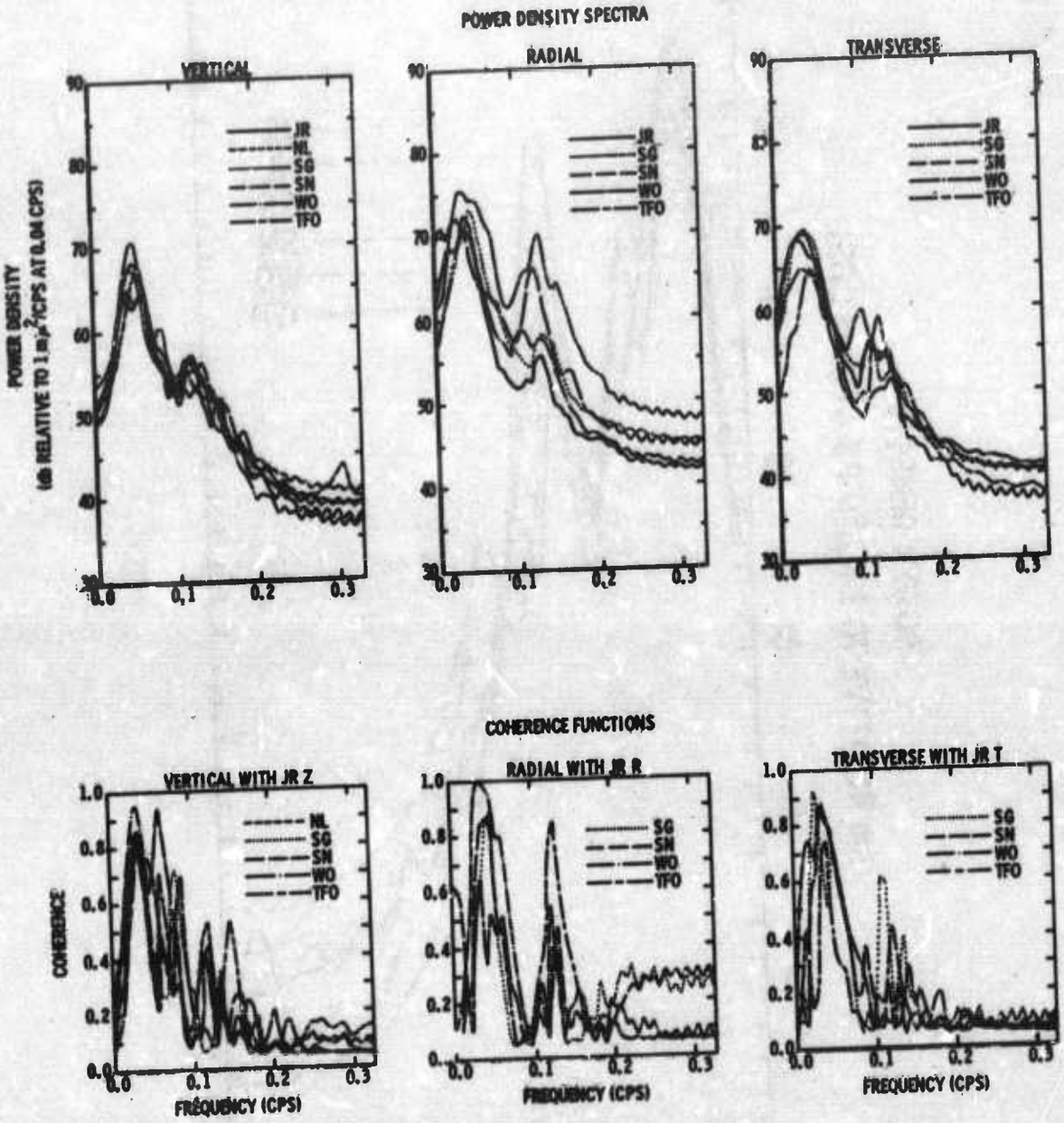

Figure IV-4. Superimposed S-Wave Power Density Spectra and Coherence Functions for Vertical, Radial and Transverse Components of Rat Islands Signal

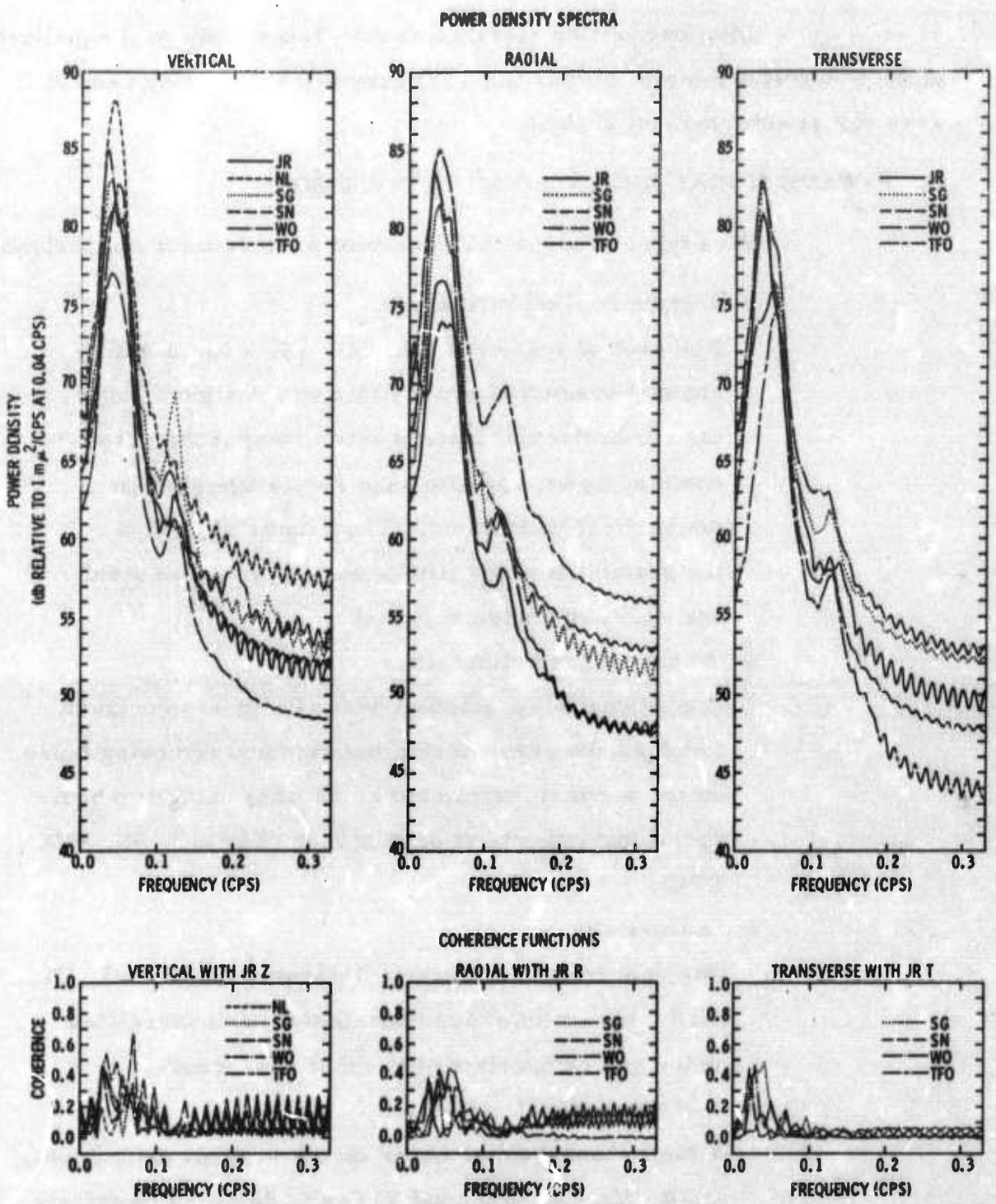

Figure IV-5. Superimposed L-Wave Power Density Spectra and Coherence Functions for Vertical, Radial and Transverse Components of Rat Islands Signal

The long-period signals are thus sufficiently well equalized in the P-wavelet interval across the TFO extended array to be used in P-wave signal enhancement studies.

B. P-WAVE SIGNAL ENHANCEMENT PROCESSORS

Five types of signal enhancement processors were analyzed:

- 3-channel prediction error
  For each of four vans (JR, SG, SN, WO), a multichannel prediction error filter was designed using the two horizontal instruments to output the error obtained by interpolating and removing noise on the vertical instrument. The outputs of each of the prediction error filters were summed to yield any additional noise rejection.
- 9-channel prediction error
  A multichannel prediction error filter was designed to output the error in interpolating and removing noise on the vertical instrument at SG when using two horizontal instruments at each of four vans (SG, SN, WO, TFO).
- Beam-steer
  The data from four vertical instruments (JR, SG, SN, WO) were summed for cancellation of uncorrelated noise and comparison with other processors.
- 5-channel signal extraction
  A multichannel filter based on the vertical instruments at JR, SG, SN, WO, and TFO was designed to extract the signal on the vertical instrument at JR.

- 9-channel signal extraction
  A multichannel filter based on data from the 3-component systems at JR, SN and WO was designed to extract the signal on the vertical instrument at JR.

The design of the P-wave signal enhancement processors was based on measured noise statistics while the signal extraction filters used a theoretical infinite velocity signal model. A constant signal-to-noise ratio of four was used for the signal model. The P-wave arrival of the signal had been previously time-aligned and appeared to be of infinite velocity.

Correlations of ±24 lags (±36 sec) in length computed over a 900-point (1350-sec) interval of noise were deconvolved with a 9-point (13.5-sec) whitening filter. The theoretical signal model was assumed to be identical for all vertical components and was built from the whitened JR van autocorrelation, while the horizontal autocorrelations and crosscorrelations between vertical and horizontal components were set to zero. Twenty-five point (37.5-sec) multichannel signal enhancement processors for both signal extraction and noise interpolation were designed and applied.

Multichannel prediction error (MPE) filters were designed to interpolate and remove the noise on the vertical instruments at each of four vans (JR, SG, SN, WO), using their respective horizontal instruments, and on the vertical instrument at SG using the horizontals at SG, SN, WO, and TFO. Displays for each filter are shown in Figures IV-6 through IV-10. For each filter the input, the MPE output, the difference traces (i.e., the interpolated noise) for the noise sample, and the vertical and MPE output traces for the signal are displayed.

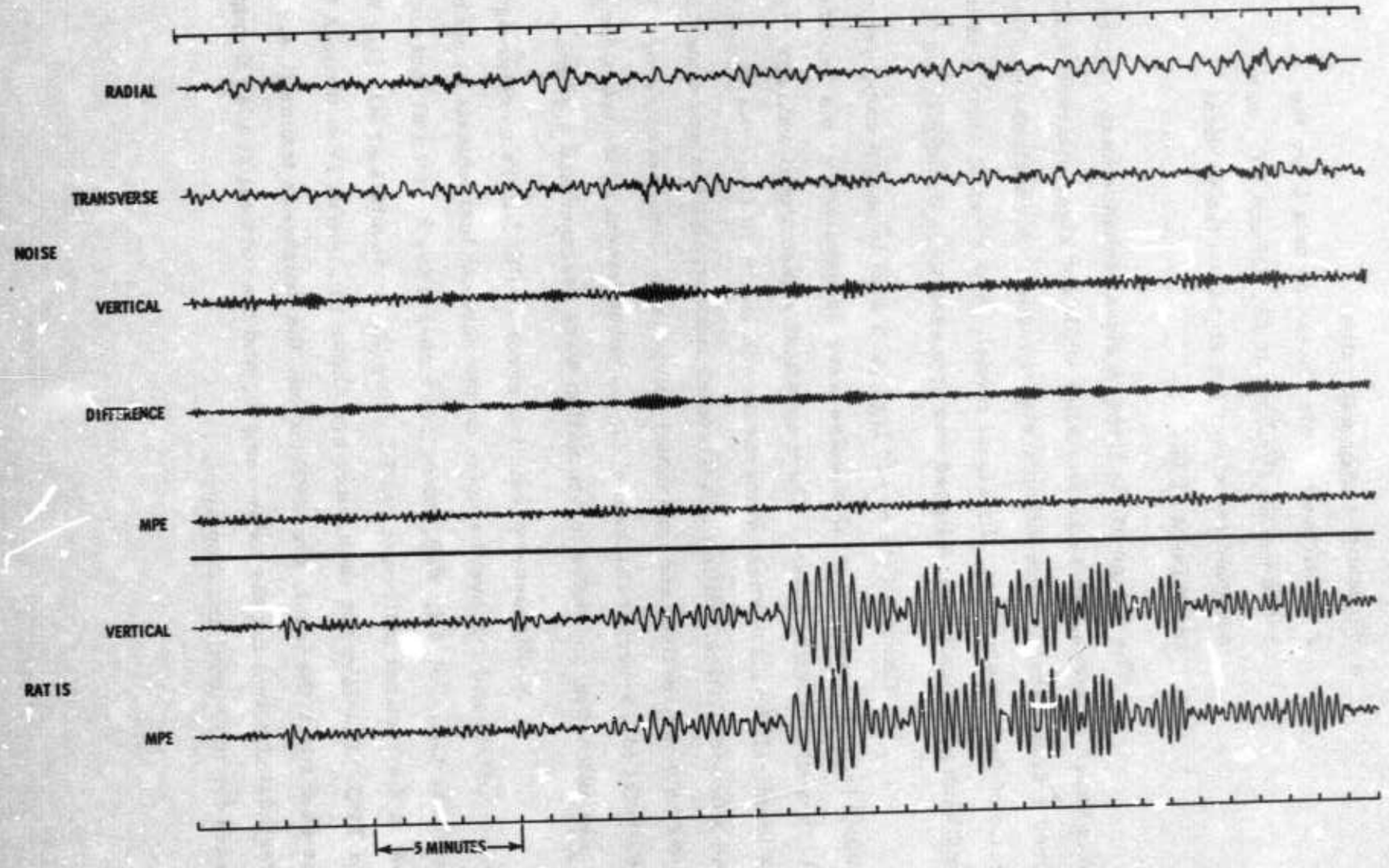

Figure IV-6. Results of Interpolating for JR Z Noise (3-Channel)

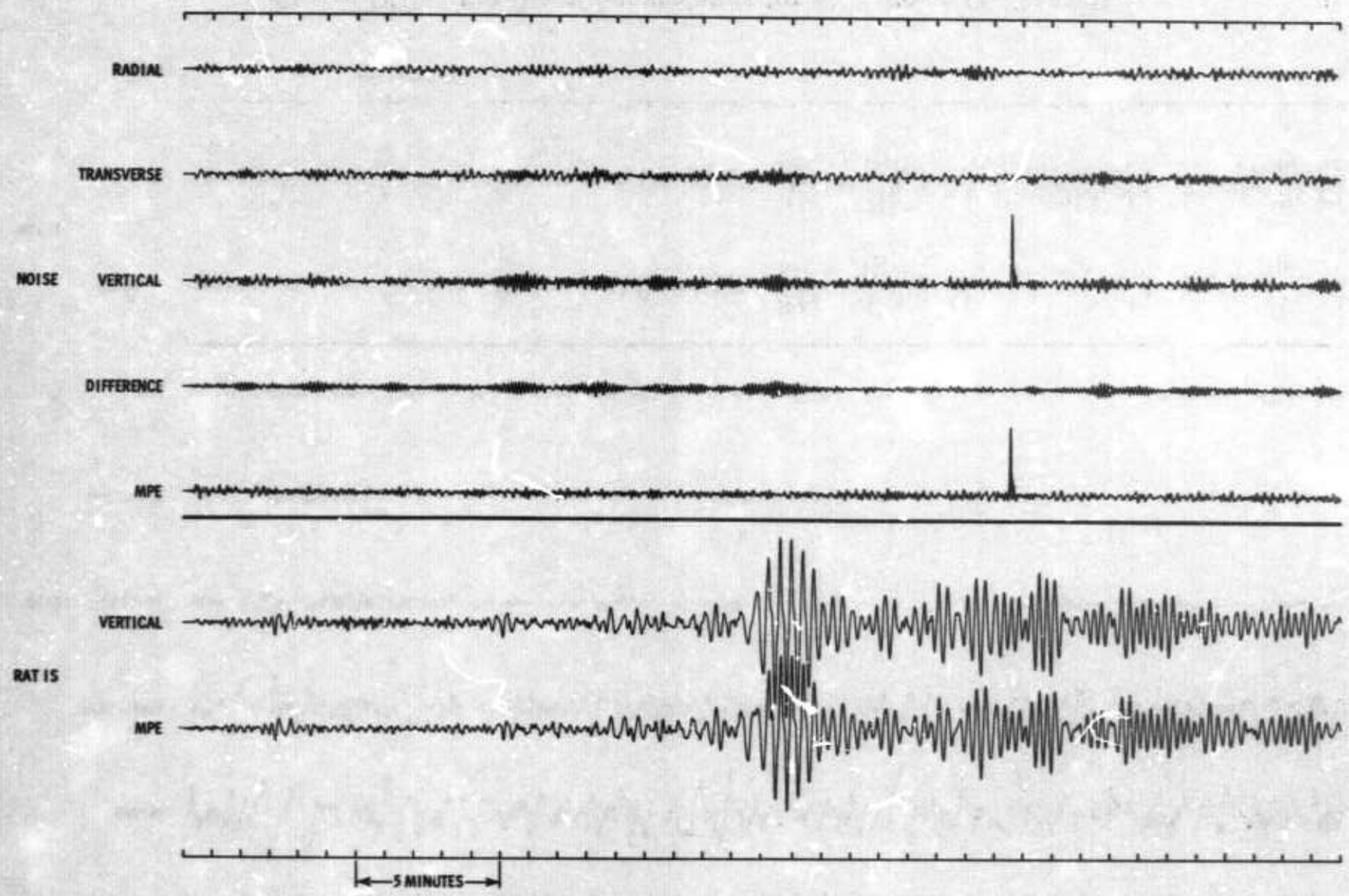

Figure IV-7. Results of Interpolating for SG Z Noise (3-Channel)

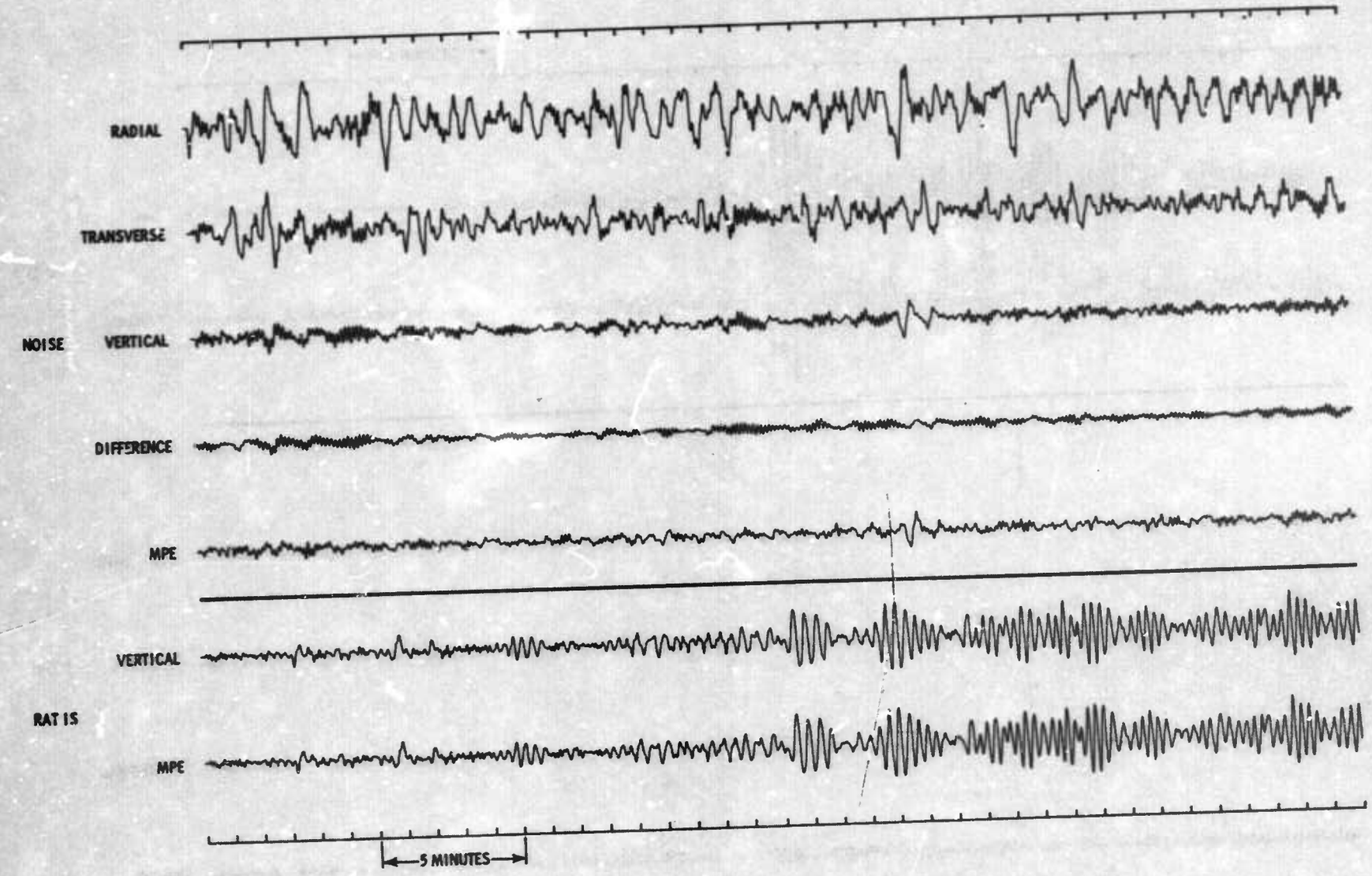

Figure IV-8. Results of Interpolating for SN Z Noise (3-Channel)

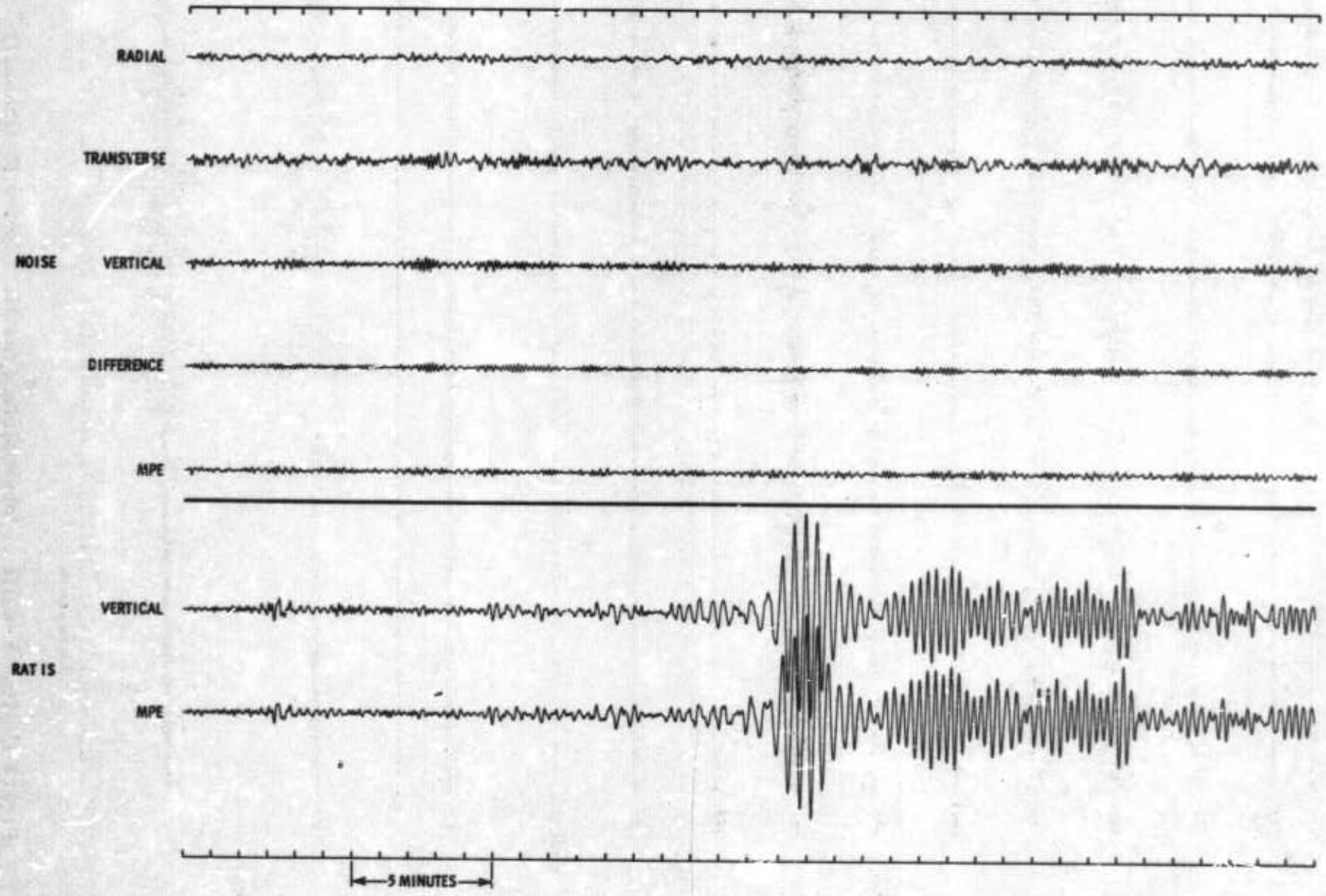

Figure IV-9. Results of Interpolating for WO Z Noise (3-Channel)

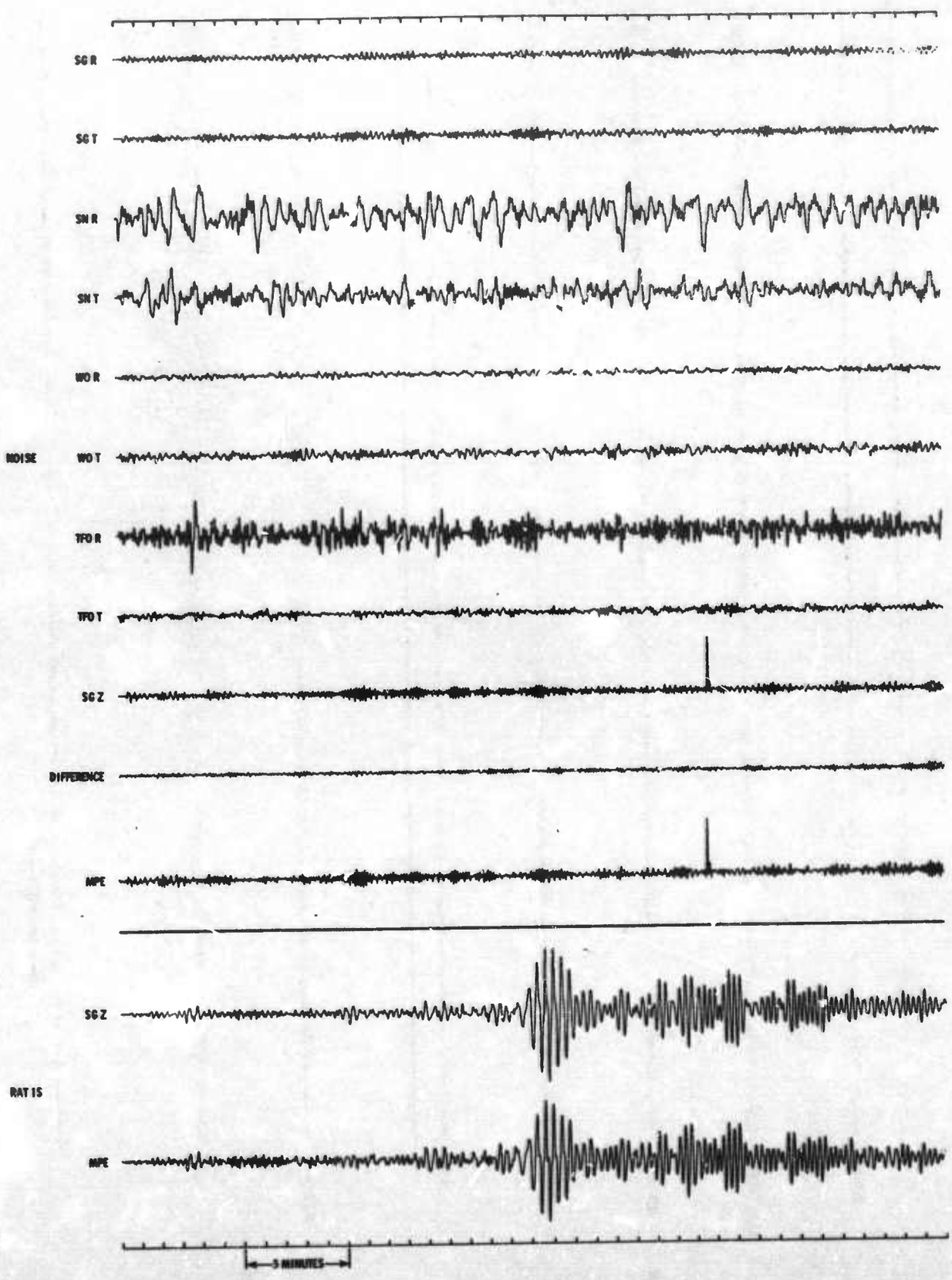

Figure IV-10. Results of Interpolating for SG Z Noise (9-Channel)

The MPE filters were designed from the first 900 points (1350 sec) of the noise sample but were applied to the entire 1600 points (2400 sec) of noise in order to evaluate the effectiveness of the filter both in and adjacent to the design interval (i.e., design and off-design intervals).

The power in the MPE output trace is an estimate of the power in the vertical trace that could not be interpolated from the horizontals. It is possible to define a "predictability" function as [1-(MPE output power)/(vertical input power)]. The function describes the fraction by which the vertical input noise power is reduced by removing the interpolated noise estimate.

Power density spectra were computed from 49-point correlations calculated over 900-point (1350-sec) and 600-point (900-sec) gates in the design and off-design noise intervals, respectively. Figure IV-11 displays "predictability" functions calculated from the power density spectra and indicates that the noise is reasonably predictable between the vertical and horizontal components over the usable seismic band and highly predictable around 0.12 cps. The predictability function for the 8-channel MPE filter, which is also shown in Figure IV-11, confirms the conclusion that the noise is essentially incoherent between the horizontal components used in this analysis.

In order to evaluate the effectiveness of the 5-channel and 9-channel signal extraction and beam-steer processors, ratios of the output noise power to the input noise power were computed from 49-point correlations over gates for both design and off-design noise areas. These ratios represent the signal-to-noise improvement possible over these noise samples, assuming no signal distortion. Insufficient noise to evaluate noise rejection for the signal samples preceded the signal onsets. In order

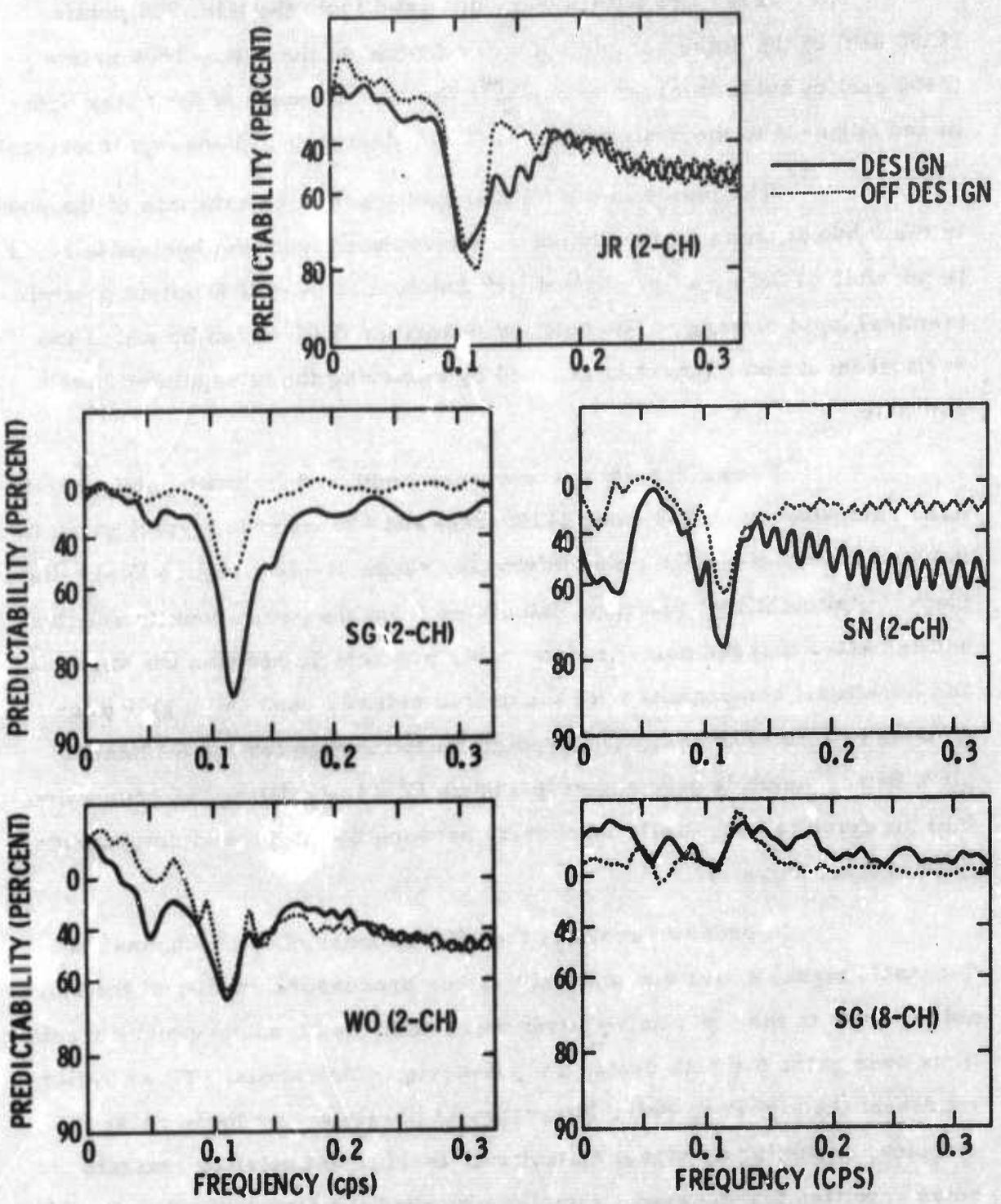

Figure IV-11. Predictability Functions

to establish the signal gain of the filters, ratios of output P-wave signal power to input P-wave signal power were computed for total correlations over a 50-point gate encompassing the P-wave. Values of the signal power ratios outside the frequency range of maximum signal power (0.04 to 0.07 cps) are probably not meaningful estimates of signal distortion due to the contamination of the transient signal waveform with ambient noise.

Results of beam-steering the four input vertical components and the four 3-channel MPE filter outputs are displayed in Figure IV-12. Appropriate noise and signal power ratios for each beam-steer case, using the JR seismometer as a reference, are shown in Figure IV-13. The theoretical maximum noise rejection ($\sqrt{n}$ in amplitude, assuming a Gaussian distribution of noise on n channels) achievable by summing a 4-channel system consisting of totally uncorrelated noise is 6 db. Figure IV-13 indicates that over the usable seismic band, except at frequencies less than 0.05 cps, the beam-steer of the input vertical traces achieved a noise reduction of about 6 db and the beam-steered MPE outputs achieved an 8 db noise reduction overall. Around 0.12 cps, the beam-steer (BS) output attains 9 db rejection and the beam-steered MPE (BS MPE) output shows 12 db rejection due primarily to vertical-horizontal coherence at this frequency. Each process caused an apparent signal loss of approximately 1 db at maximum signal power (near 0.04 cps) due to contamination of the transient signal with ambient noise, misalignment and slight inequalization residuals of the P-wave. The deviation of the off-design power ratio from the design area ratio is caused by a spike on the SG van data in the off-design interval.

Figure IV-14 displays the impulse response for an infinite velocity, vertically-arriving compressional impulse of unit gain of the 5-channel signal extraction MCF and its amplitude and phase response. The 9-channel response (not shown) to an infinite velocity, vertically-arriving compressional impulse of unit gain is very similar. Results of

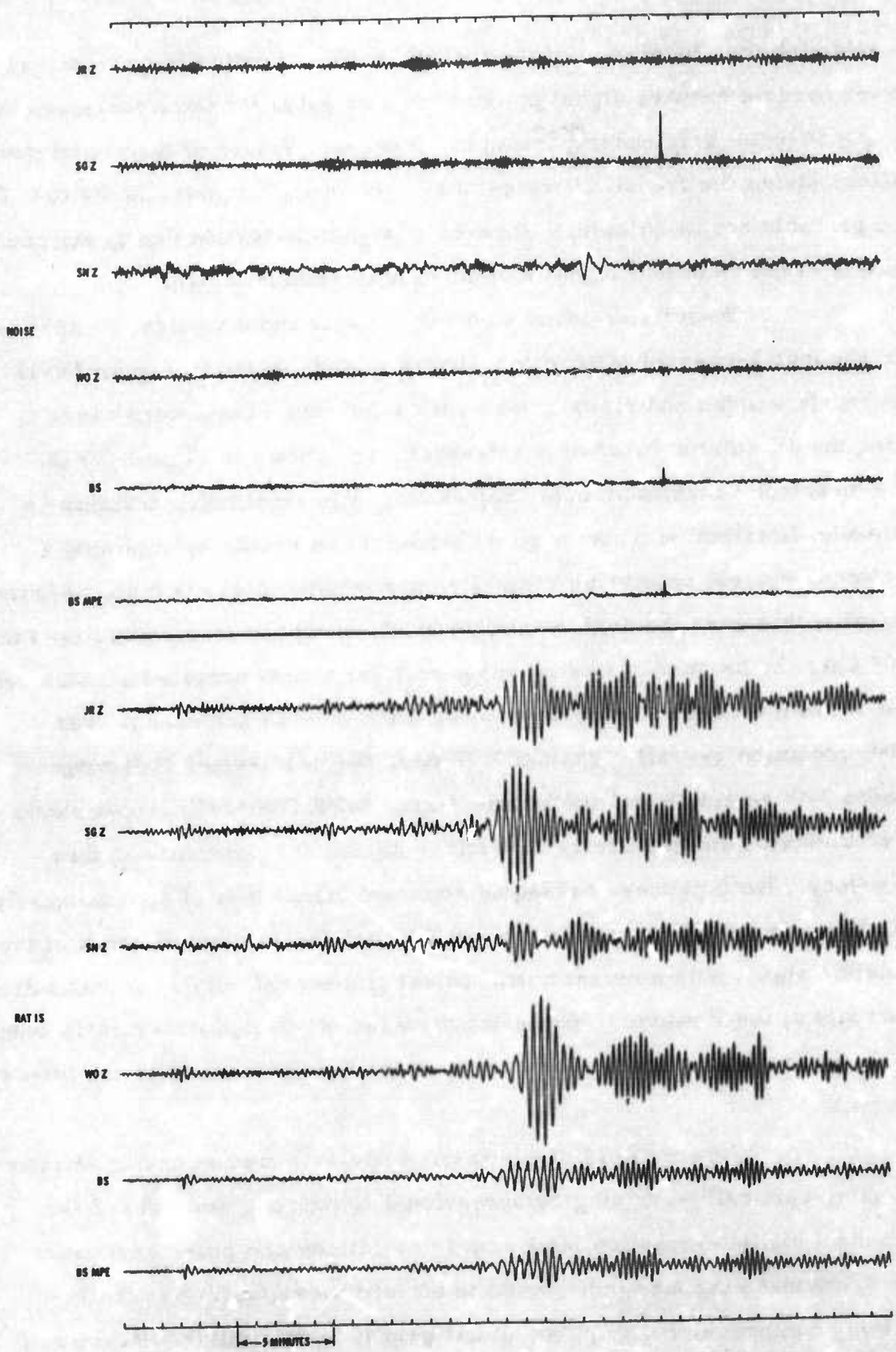

Figure IV-12. Results of Beam-Steering

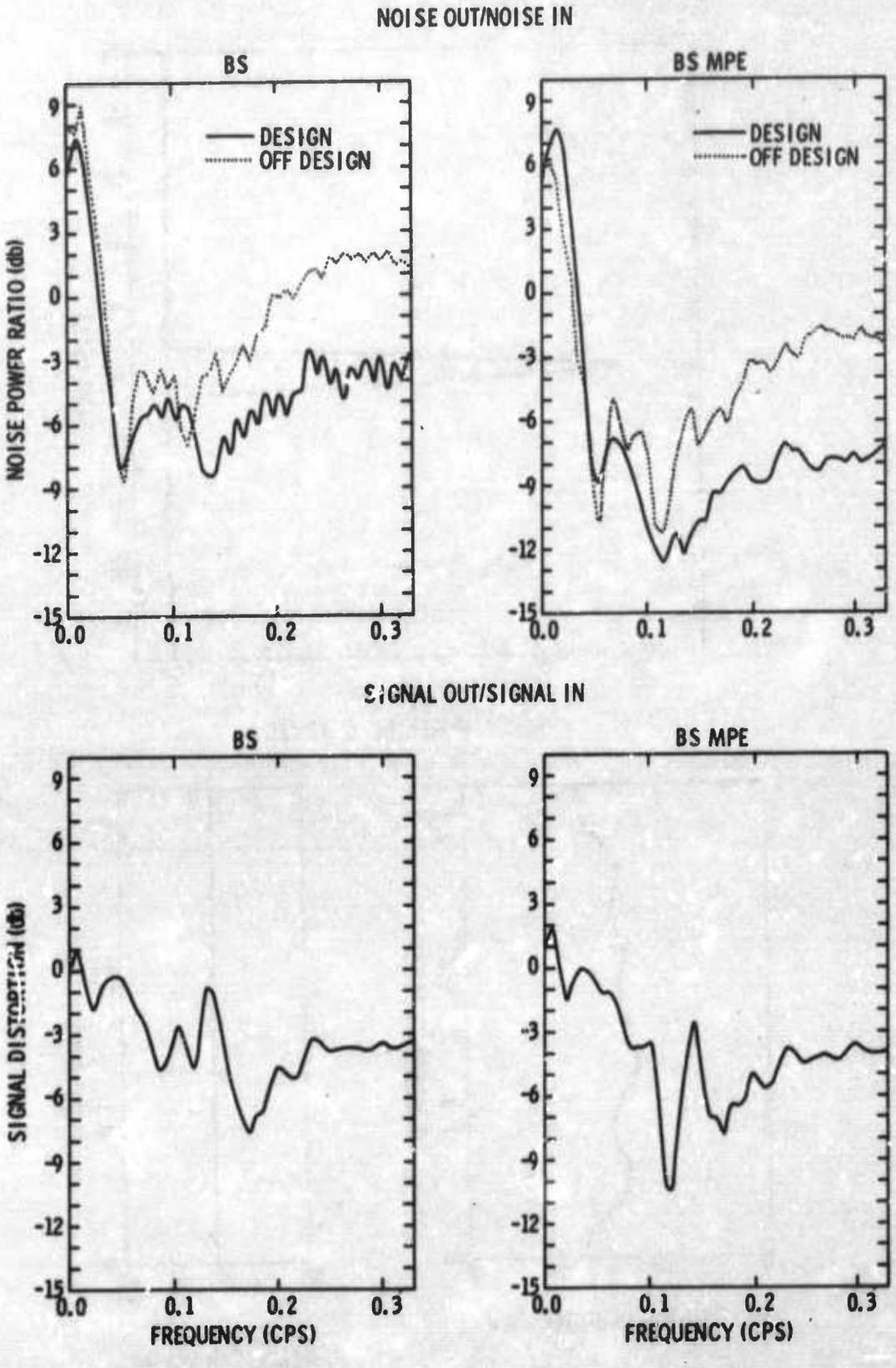

Figure IV-13. Noise and Signal Power Ratios for Beam-Steering

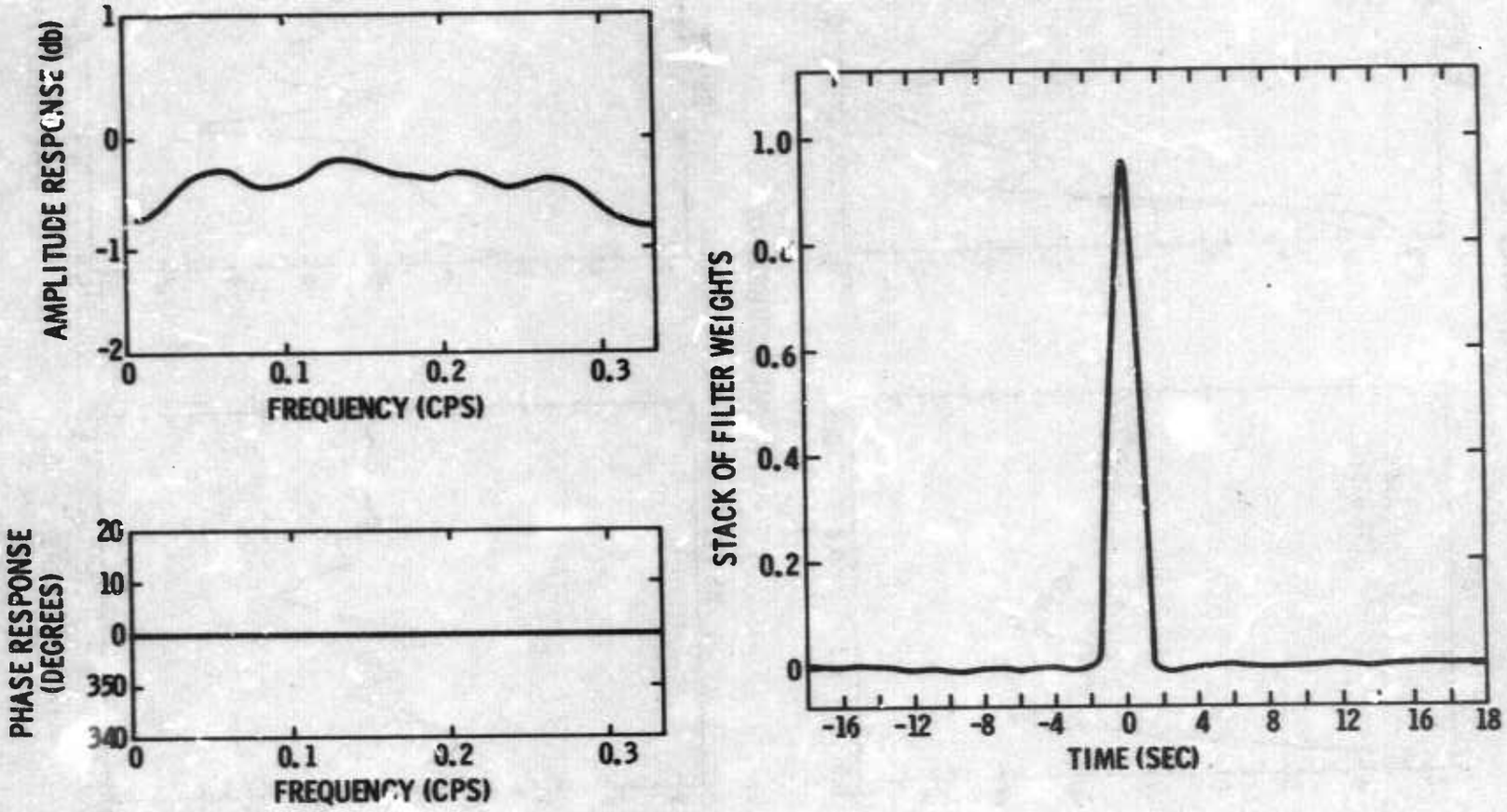

Figure IV-14. Response of 5-Channel Signal Extraction Filter

applying the 5-channel and 9-channel MCF's are shown in Figure IV-15 and IV-16 and their corresponding power ratios are displayed in Figures IV-17 and IV-18. At frequencies greater than 0.05 cps, the 5-channel MCF noise rejection is generally on the order of $\sqrt{n}$ (7 db). Again, the deviation of the off-design noise ratio is due to a spike on SG. The 9-channel MCF exceeded (12 db at 0.12 cps) the random noise improvement (10 db) at certain frequencies above 0.05 cps due primarily to the correlated nature of the horizontal and vertical noise at these frequencies. The off-design noise ratio has less rejection due to an apparent change in the noise character on the horizontal instruments. Both MCF's had signal distortion at 0.04 cps in the order of 1 db which slightly exceeds that indicated by the amplitude responses of the filters and which is probably due to contamination of the signal estimate, P-wave misalignment and slight inequalization residuals. Figure IV-19 displays a comparison of the signal enhancement processor outputs for the signal and noise samples.

In summary, the 3-component signal enhancement processors performed satisfactorily and achieved noise rejection generally greater than $\sqrt{n}$ for frequencies above 0.05 cps and especially around 0.12 cps. This was due primarily to the correlated properties of the noise field between vertical and horizontal components.

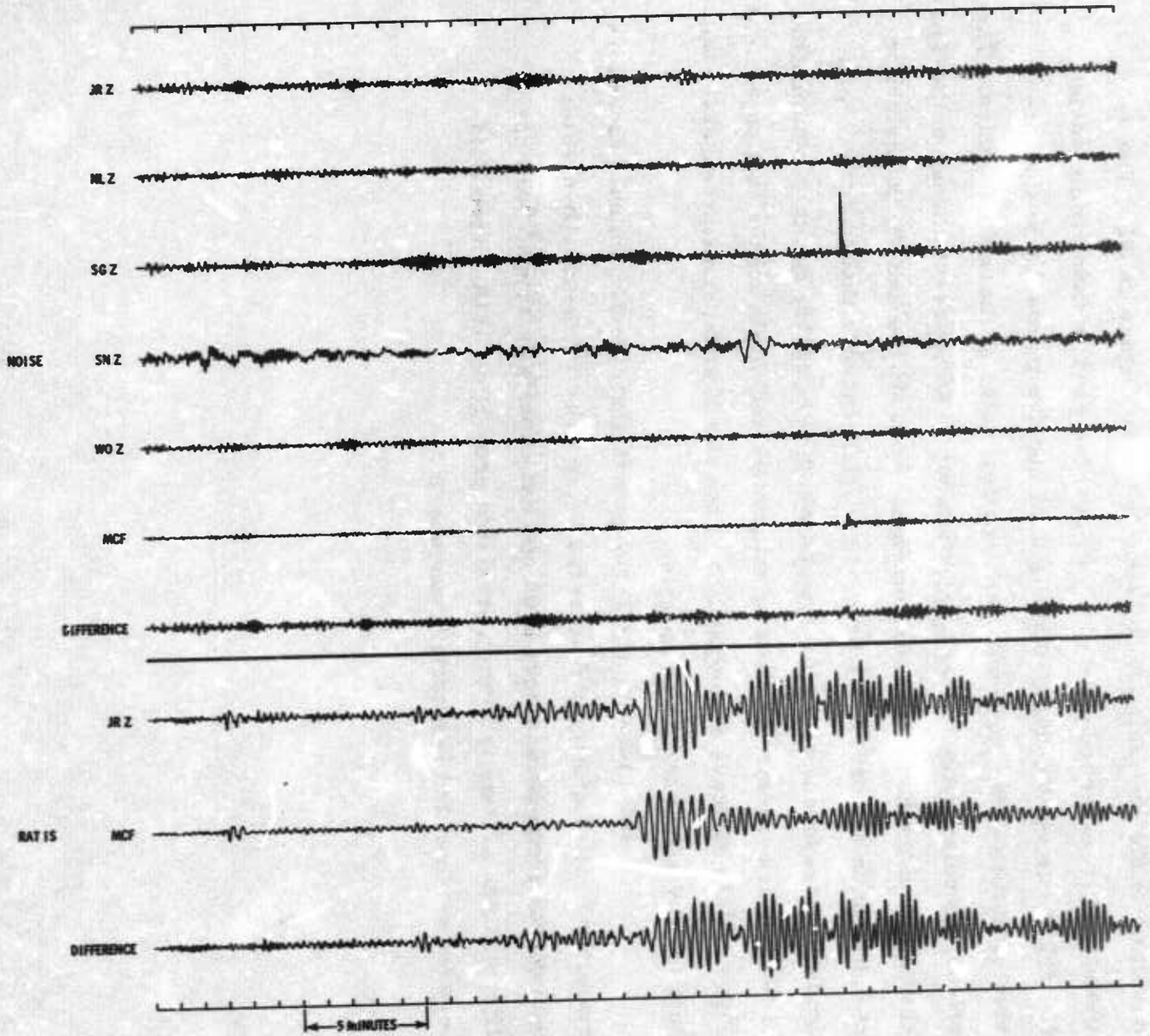

Figure IV-15. Results of Applying 5-Channel MCF

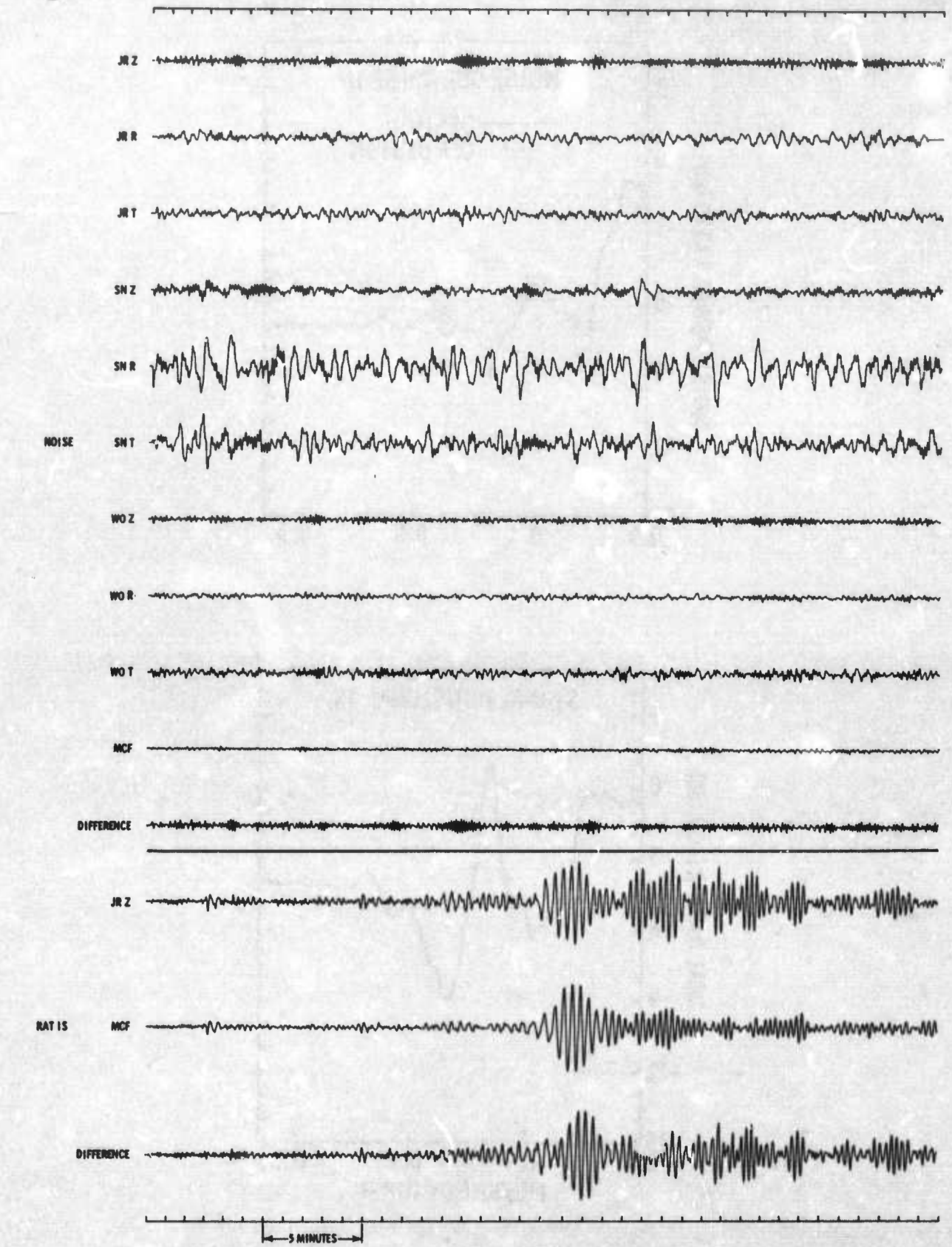

Figure IV-16. Results of Applying 9-Channel MCF

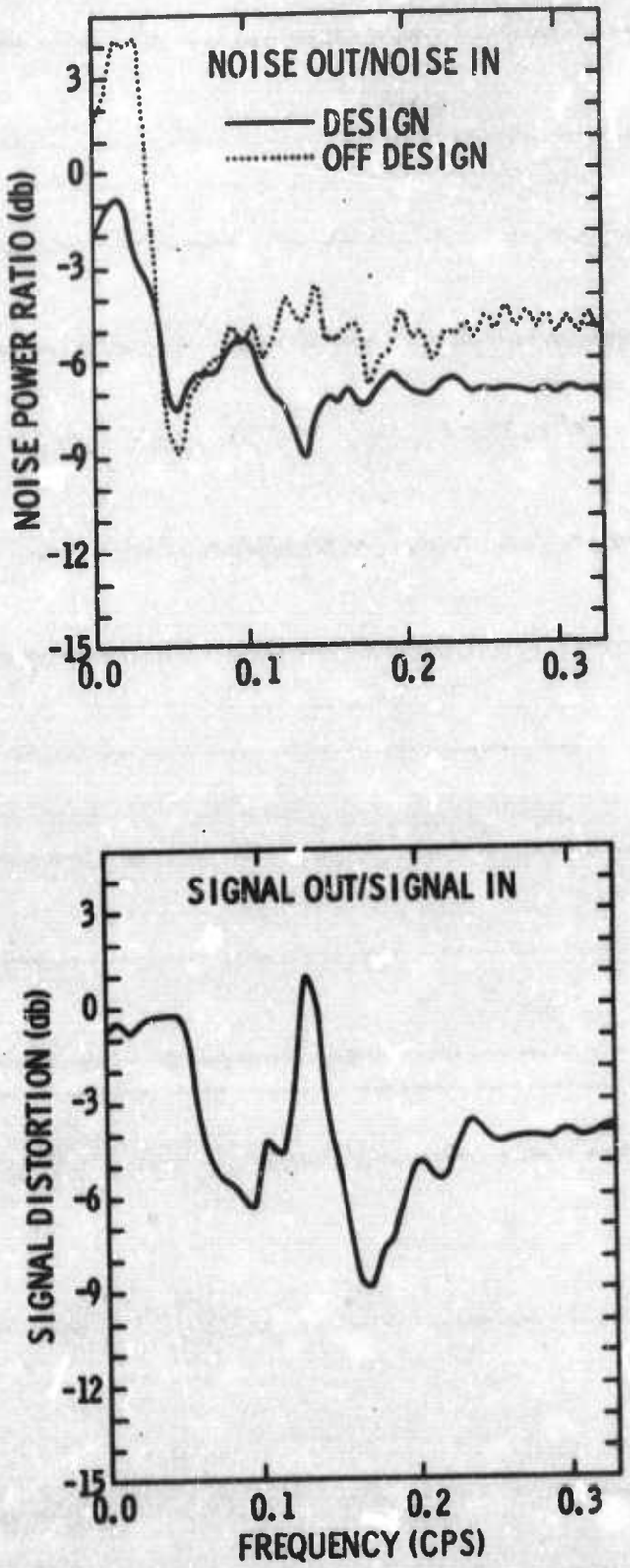

Figure IV-17. Noise and Signal Power Ratios for 5-Channel MCF

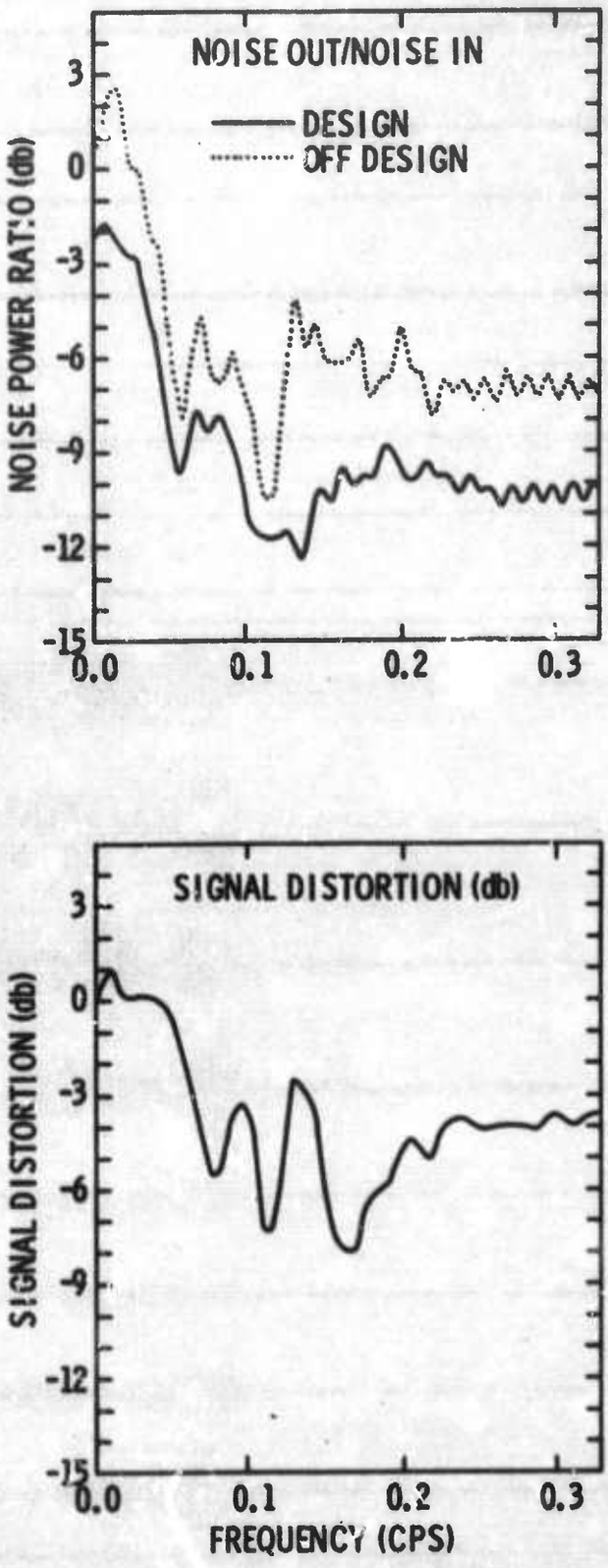

Figure IV-18. Noise and Signal Power Ratios for 9-Channel MCF

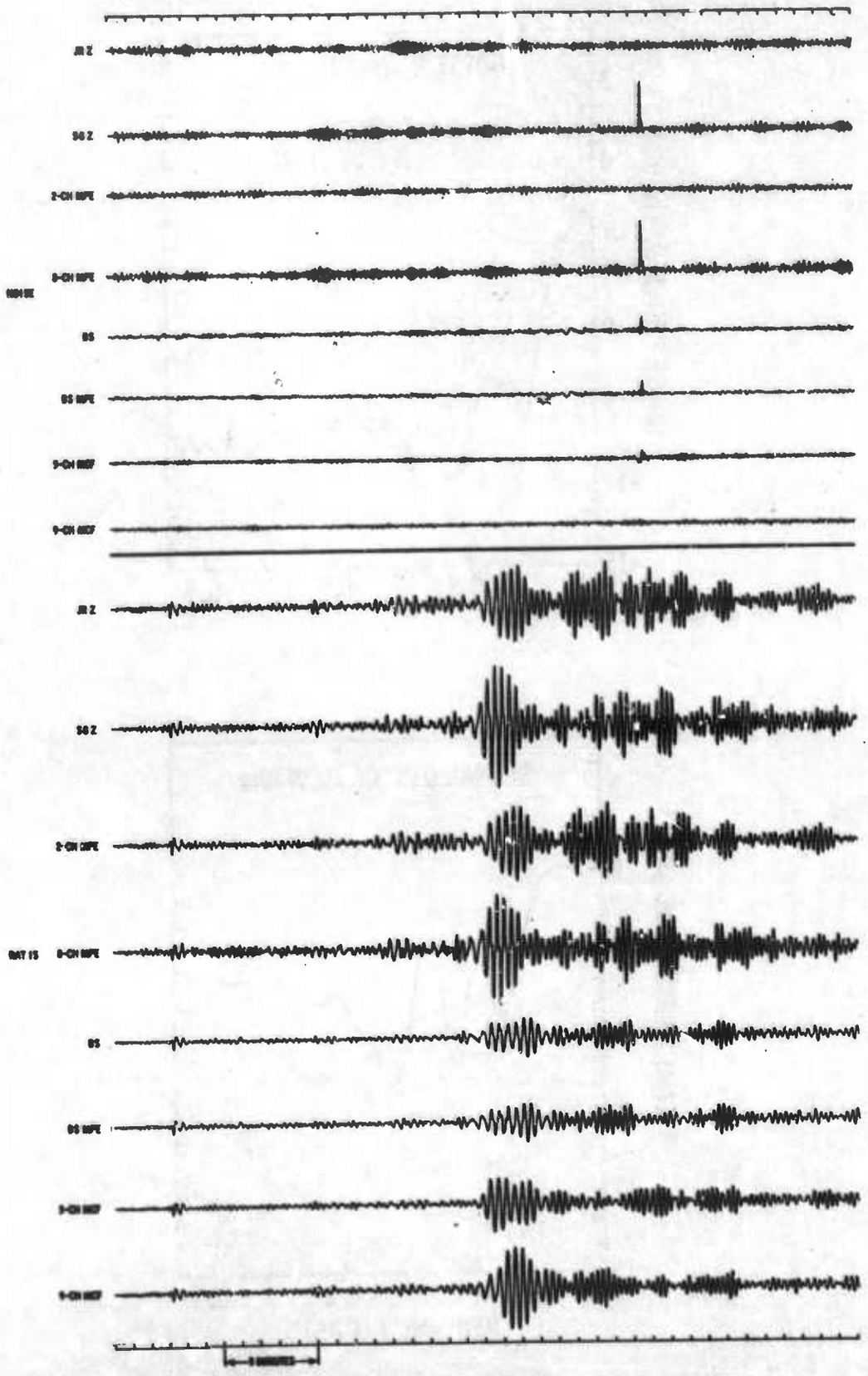

Figure IV-19. Comparison of Long-Period Signal Enhancement Processors

SECTION V

3-COMPONENT SHORT-PERIOD DATA ANALYSIS

This section describes in detail the analysis and results of signal equalization and P-wave signal enhancement processor studies conducted with the TFO short-period 3-component crossarray. Figure V-1 shows the location and orientation of the 3-component instruments. An indication of the wide variations in geology over the array was shown in Figure IV-2.

The ambient seismic noise field statistics have been investigated previously on a 3-component basis in the short-period frequency range.[4] Over the usable seismic bandwidth of approximately 0.1 to 1.3 cps, noise is essentially uncorrelated for a 10-km seismometer separation except for the dominant Rayleigh wave energy peak in the 4- to 6-sec microseism band, which seems reasonably time- and space-stationary. Results similar to those for this study were previously reported for seismometer spacings in the order of 4 km (Semiannual Technical Report No. 3).[5] The analysis of the TFO short-period data has been hindered, as far as absolute measurements are concerned, by the apparently unreliable gain corrections (Semiannual Technical Report No. 5).[6]

A. SIGNAL EQUALIZATION STUDIES

For effective teleseismic signal enhancement, it is essential that signal waveforms be reproducible at all observation points within an array. Signal equalization across the TFO array was examined for the two signals described in Section III. Only the locations (Z61, Z68, Z13) selected for use in the signal enhancement studies were analyzed.

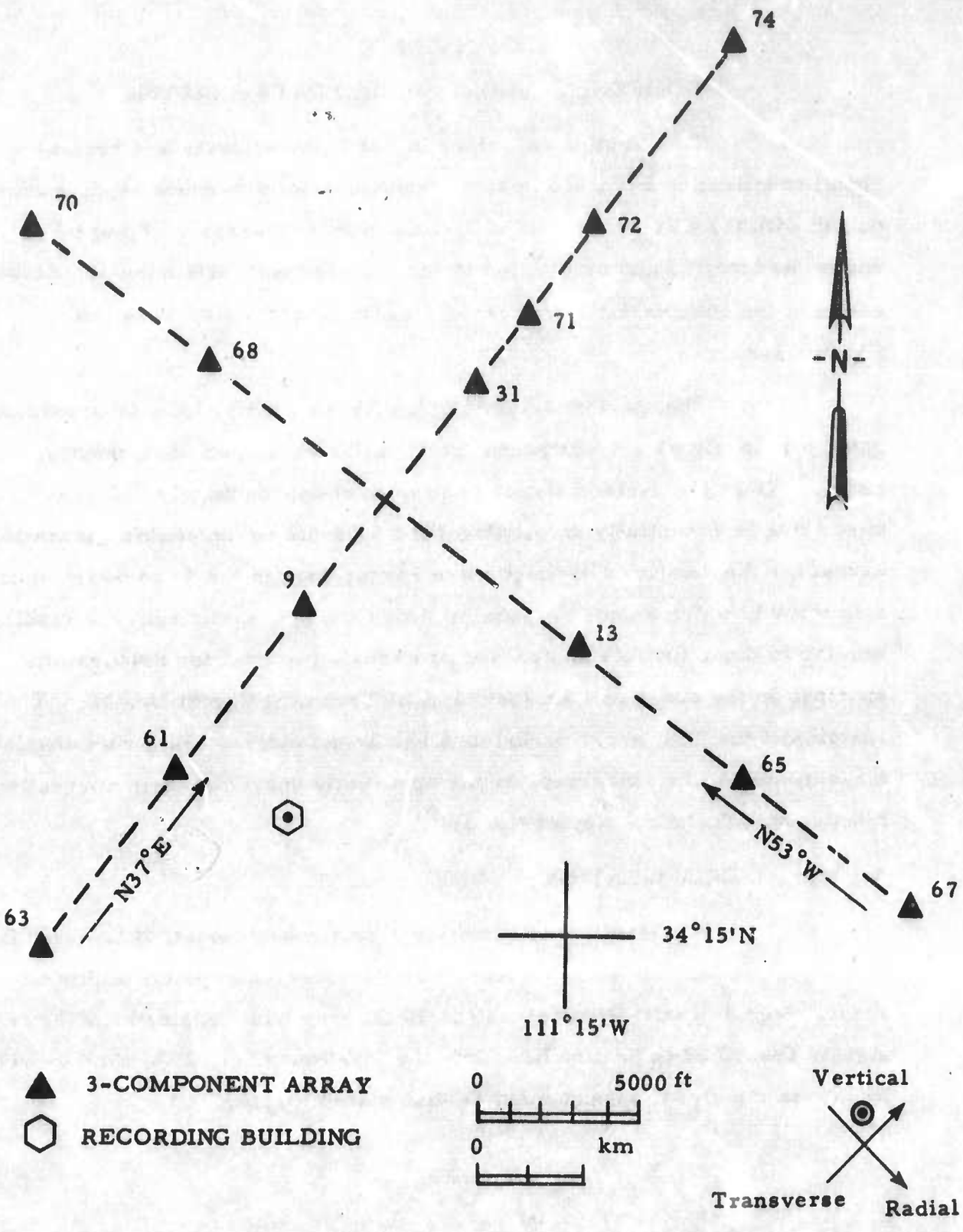

Figure V-1. TFO 3-Component Short-Period Seismometer Locations

Visual examination of the recorded waveforms (Figure III-3) suggests that they are reasonably reproducible across the array. The reproducibility of the P phase is shown quantitatively with power density spectra and with 2-channel coherence functions in Figure V-2. It is also shown by 50-point crosscorrelation functions (Figure V-3) computed over a 100-point (10-sec) gate encompassing the P-wave onset.

The close agreement of the power density spectra (±2 db) for the vertical instruments over the usable seismic bandwidth indicates that crustal filtering causes little variation and suggests that the signal vertical component magnification compensations (derived from on-site calibrations) were reasonably correct for these signals. Coherence is high over the interval of peak power; values outside this frequency range are probably not meaningful estimates of signal coherence. Crosscorrelation functions of perfectly reproducible signal waveforms should be identical for all pairs of instruments and should be symmetrical. These properties are closely approximated by the crosscorrelations, except for the effects of slight gain variations. The short-period P-wave signals are thus sufficiently well equalized to be used in P-wave signal enhancement studies.

B. P-WAVE SIGNAL ENHANCEMENT PROCESSORS

Three types of processors were analyzed

- 3-channel prediction error

  For each of three locations (Z61, Z68, Z13) a multi-channel prediction error filter (MPE) was designed to output the error obtained by interpolating and removing the noise present on the vertical instrument when using the two horizontal instruments. The outputs from each of the prediction error filters were summed for any additional noise rejection.

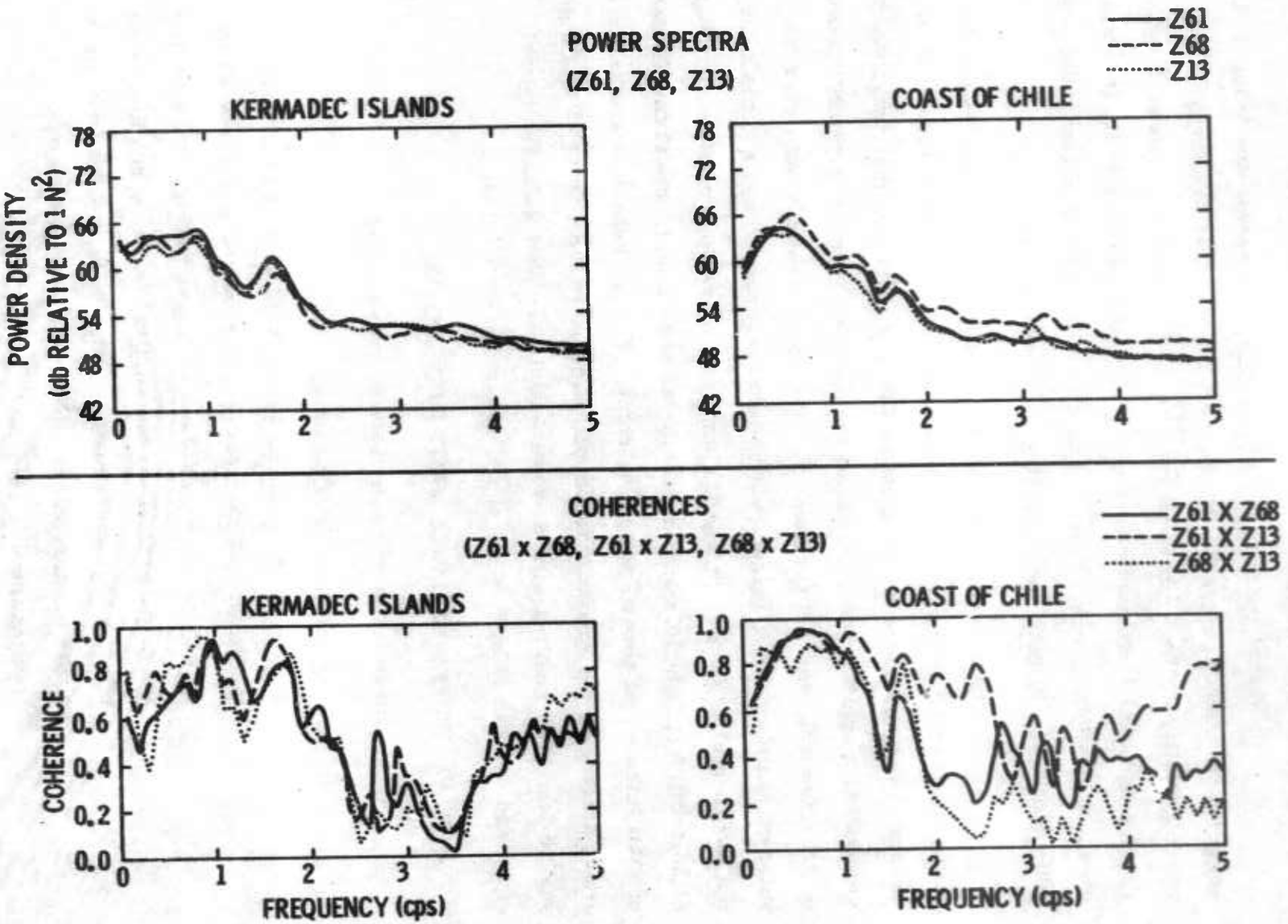

Figure V-2. Superimposed P-Wave Power Density Spectra and Coherence for Vertical Components

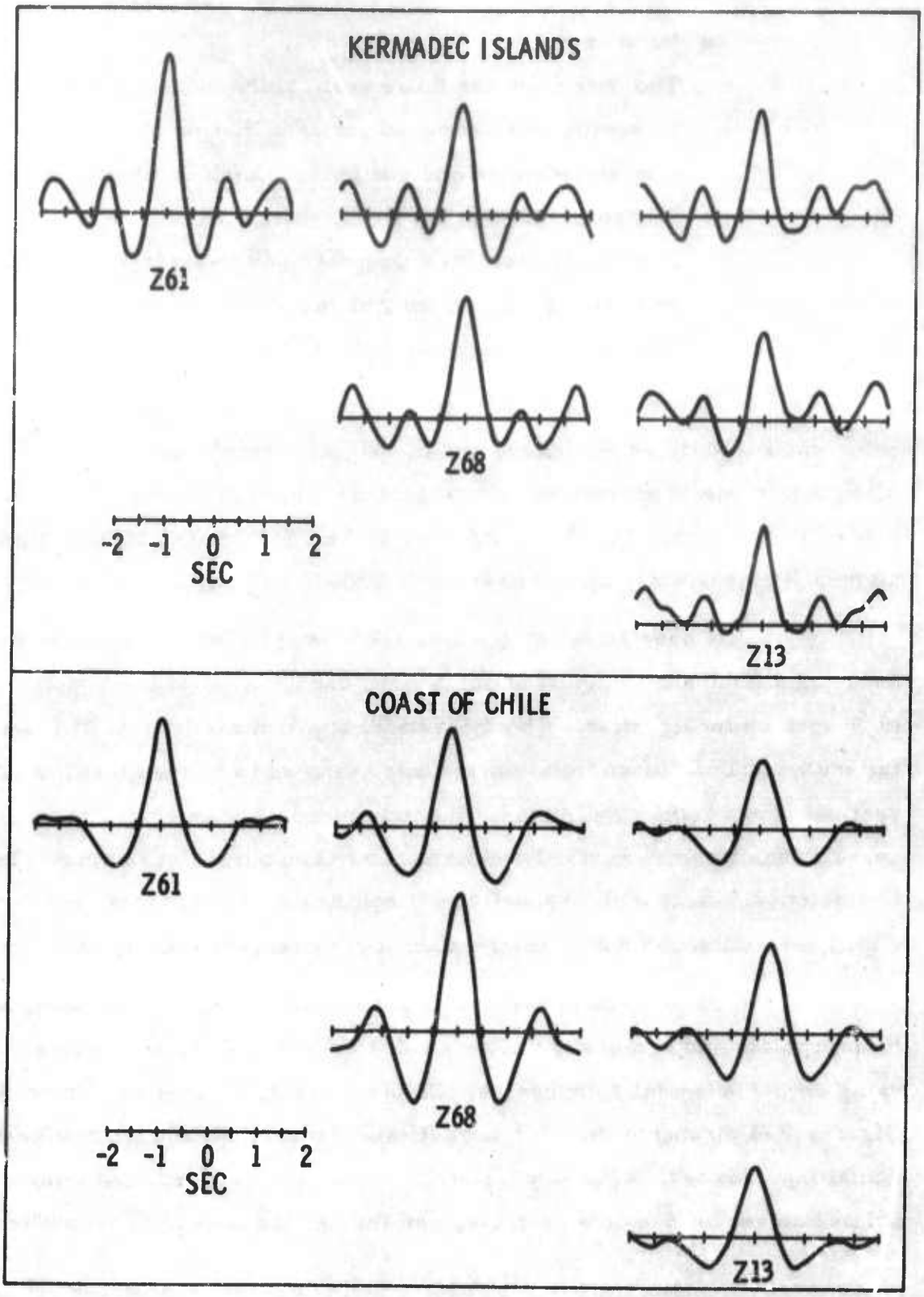

Figure V-3. Correlation Matrices for Vertical Component of Signal P-Wave

- Beam-steer
  The data from the three vertical instruments of the tripartite were summed for cancellation of uncorrelated noise and comparison with other processors.
- 9-channel (tripartite) signal extraction
  A multichannel filter was designed to extract the signal on vertical instrument Z61 based on data from the 3-component systems at Z61, Z68 and Z13.

The P-wave signal enhancement processors were designed using measured noise statistics, and the signal extraction filter was designed using a theoretical infinite velocity signal model with constant signal-to-noise ratio of four. The P-wave onsets of the two signals had been time-aligned previously and appeared to be of infinite velocity.

Correlations of ±24 lags (±2.4 sec) in length computed over a 2400-point (240-sec) interval of noise were deconvolved with a 9-point (0.9-sec) whitening filter. The theoretical signal model was built from the whitened Z61 autocorrelation and was assumed to be identical for all vertical components, while the horizontal autocorrelations and cross-correlations between vertical and horizontal components were zero. Twenty-five point (2.5-sec) multichannel signal enhancement processors for both signal extraction and noise interpolation were designed and applied.

Multichannel prediction error (MPE) filters were designed to interpolate and remove the noise on Z61, Z68 and Z13, respectively, using their horizontal components. Displays for each filter are shown in Figures V-4 through V-6. For each filter, the vertical and the two horizontal input traces, MPE output and difference traces (i.e., the interpolated noise) for the noise sample, and the vertical and MPE output traces

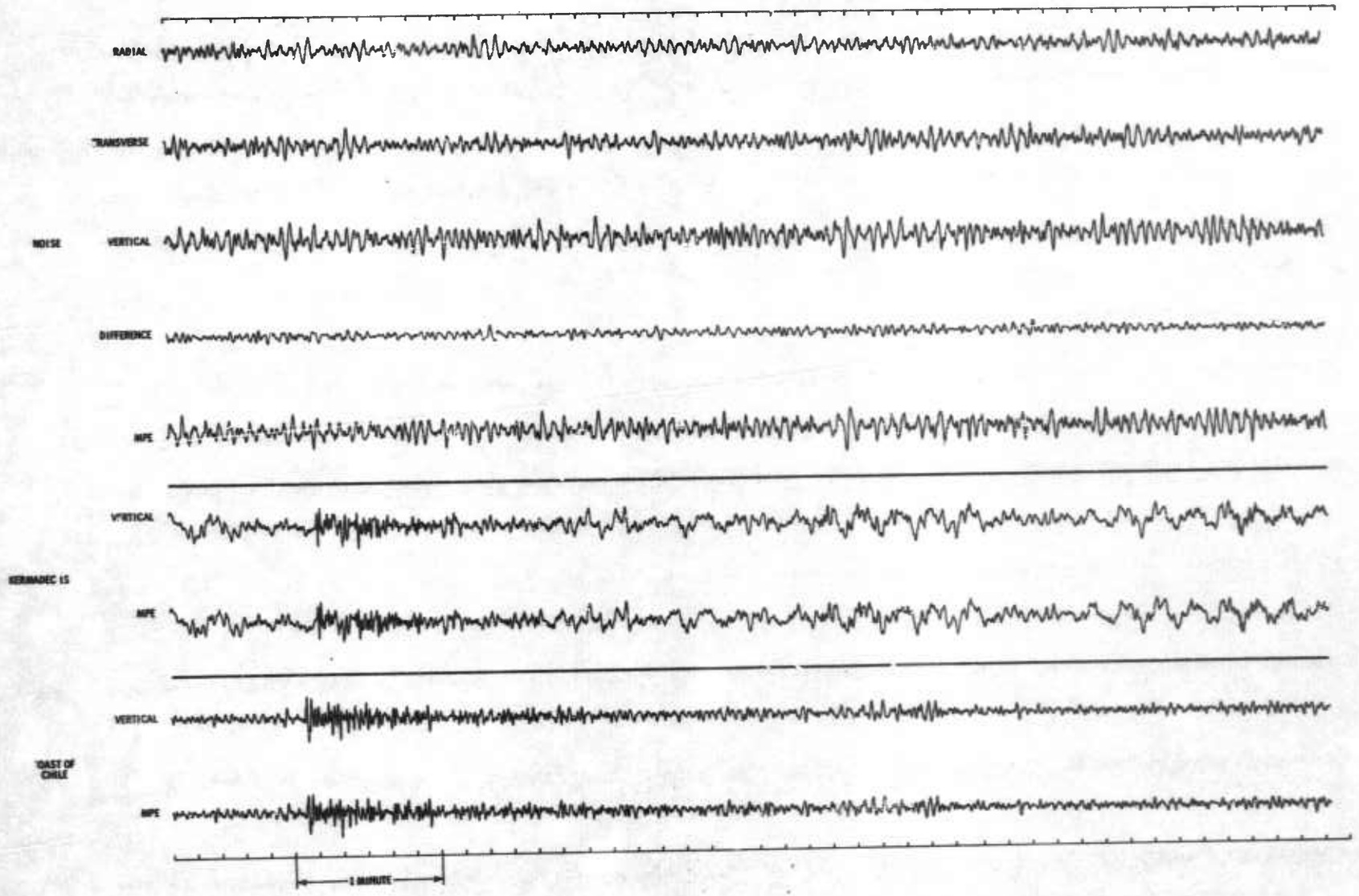

Figure V-4. Results of Interpolating for Z61 Noise

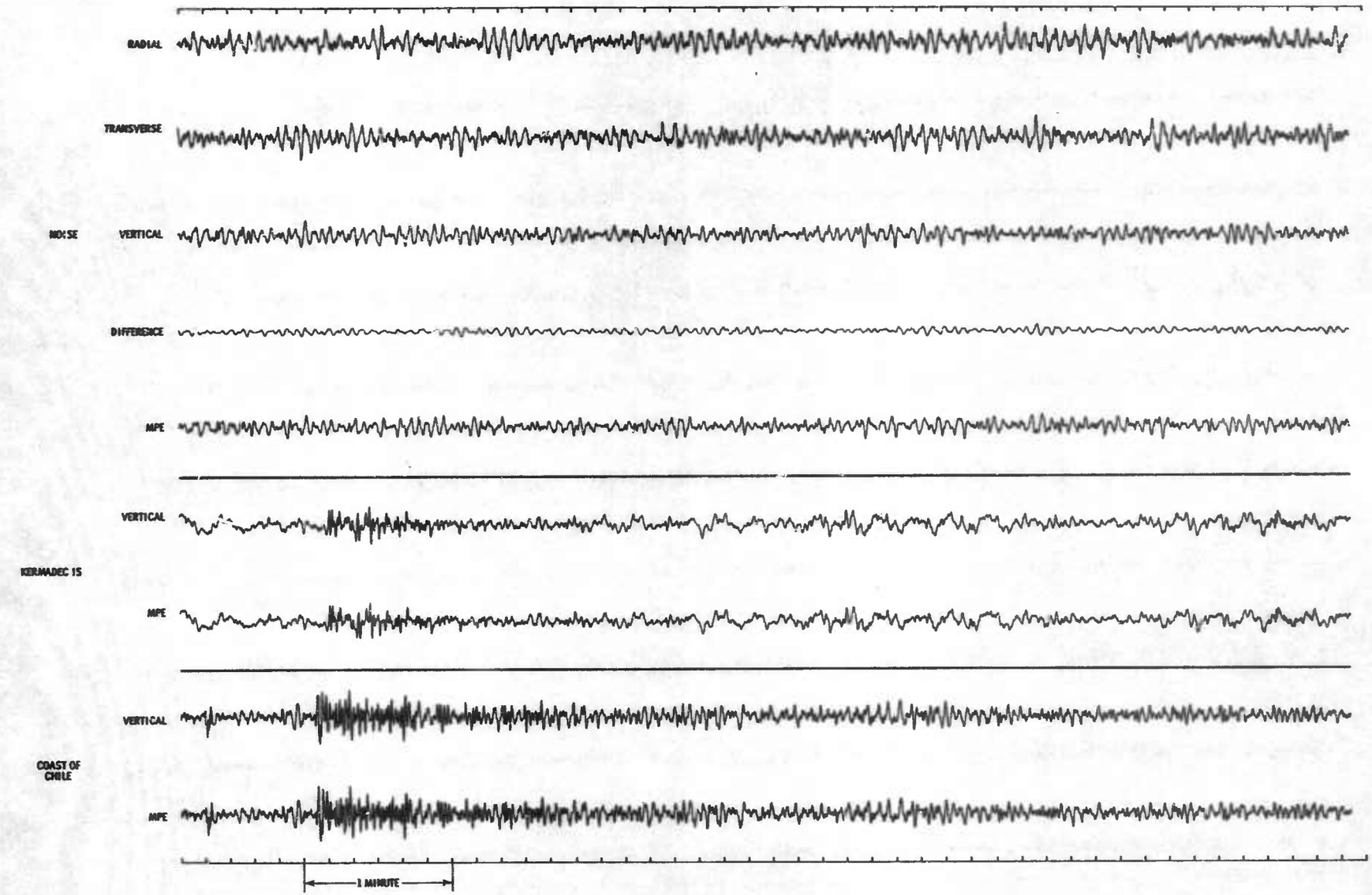

Figure V-5. Results of Interpolating for Z68 Noise

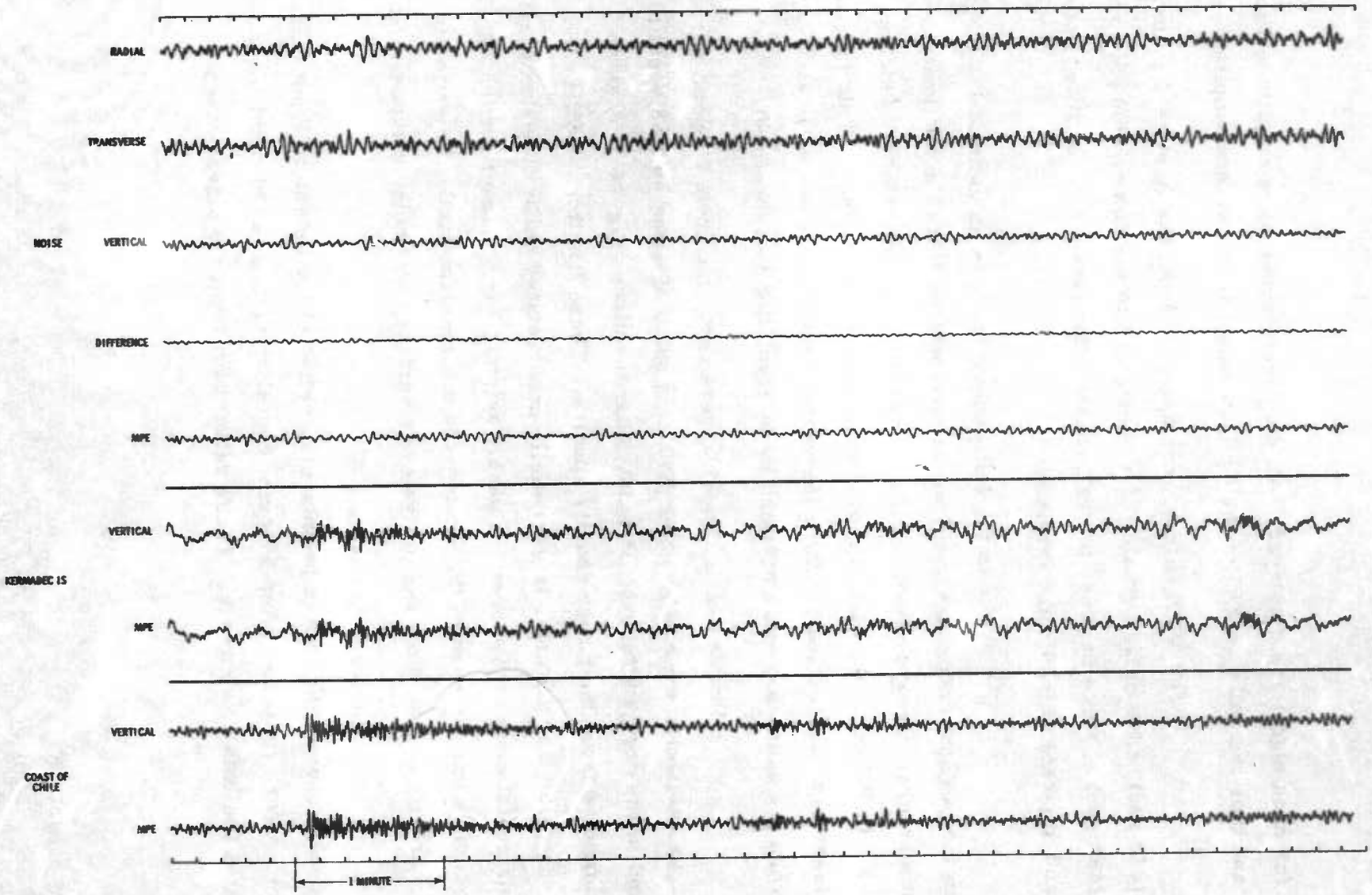

Figure V-6. Results of Interpolating for Z13 Noise

for each signal are displayed. All displayed traces were amplitude-limited, and thus the spike on Z68 of the Chilean signal is not at true amplitude.

The MPE filters were designed from the first 2400 points (240 sec) of the noise sample but were applied to the entire 4800 points (480 sec) of noise in order to evaluate the effectiveness of the filter both in and adjacent to the design interval.

The power in the MPE output trace is an estimate of the power in the vertical trace that could not be interpolated from the horizontal seismometers. Using the ratio of these powers, a "predictability" function, [1 - (MPE output power)/(vertical input power)] is defined. This function describes the fraction by which the vertical input noise power is reduced when the estimated noise obtained by interpolation is subtracted.

Power density spectra were computed from 50-point correlations calculated over 2400-point (240-sec) gates of noise both adjacent to and in the design interval. Predictability functions (Figure V-7) were computed from the power density spectra. These functions confirm the conclusion that the noise is essentially uncorrelated between vertical and horizontal components over the usable seismic band, except for the slight interpolation achieved in the 4- to 6-sec microseism band. Rejection is apparently achieved for the low velocity surface wave noise component only.

In order to evaluate the effectiveness of the 9-channel signal extraction and beam-steer processors, ratios of the output-to-input noise power were computed from 50-point correlations over 2400-point (240-sec) gates for both noise areas. These ratios represent the signal-to-noise

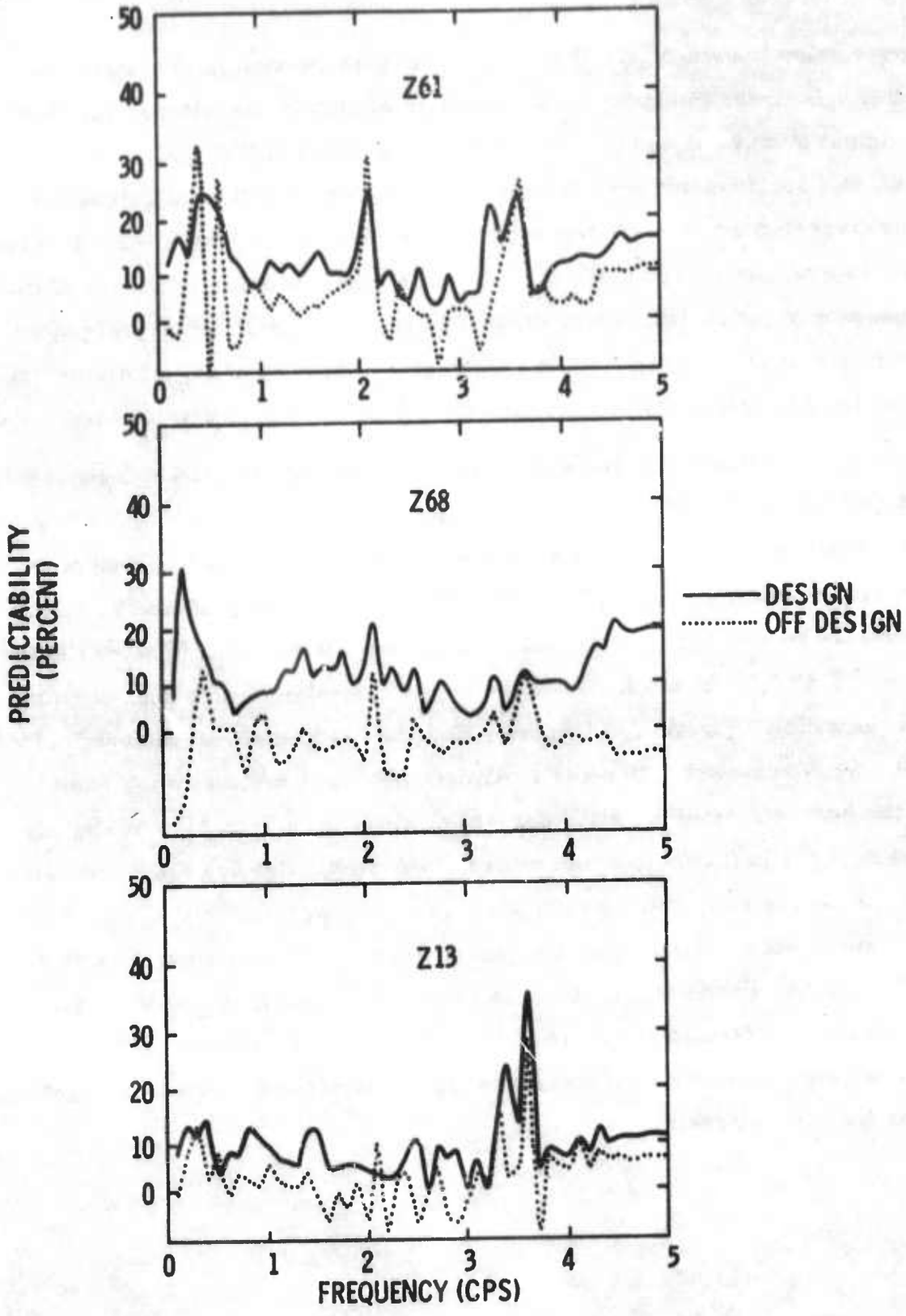

Figure V-7. Predictability of Vertical Components

improvement possible over these noise samples, assuming no signal distortion. In order to estimate the signal distortion of the filters, ratios of the output P-wave signal power to the input P-wave signal power were calculated for 50-point correlations over a 100-point (10-sec) gate which encompassed the P-wave. Not enough noise was present before the P-wave onset to evaluate noise rejection over these signal samples. Values of the signal power ratios outside the frequency range of maximum signal power (0.4 to 1.0 cps) are probably not meaningful estimates of signal distortion due to the contamination of the transient signal waveform with ambient noise.

Results of beam-steering the three input vertical components (BS) and the outputs of the three MPE filters (BS MPE) are shown in Figure V-8. Appropriate noise and signal power ratios are shown for each of the beam-steer cases in Figure V-9. The theoretical maximum noise rejection achievable by summing a 3-channel system containing totally uncorrelated noise is 5 db ($\sqrt{n}$ in amplitude, assuming a Gaussian distribution of noise on n channels). Figure V-9 indicates that the beam-steer of the vertical input traces achieved 5 db noise rejection over the usable seismic band, and the beam-steer of the MPE outputs achieved a noise rejection slightly greater (6 db) in the 4- to 6-sec microseism band. Outside the microseism band, the noise rejection for both processes is approximately equal. Both beam-steer operations caused a signal distortion of approximately 2 db for the Kermadec Islands signal and 0 db for the Chilean signal. The slight apparent signal distortion observed is probably due to contamination of the transient signal by ambient noise, misalignment of the P-wave and slight inequalization residuals.

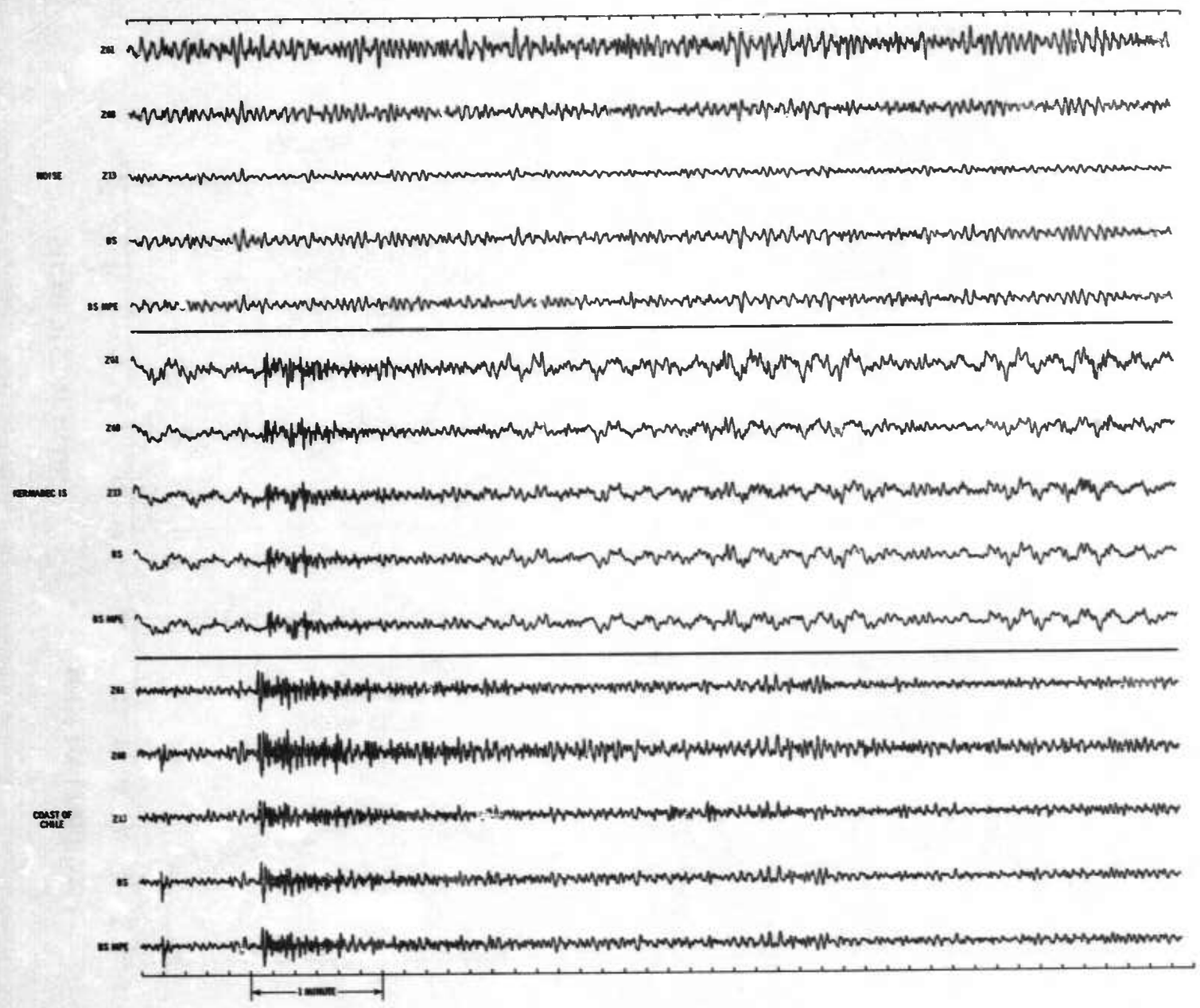

Figure V-8. Results of Beam-Steer Processors

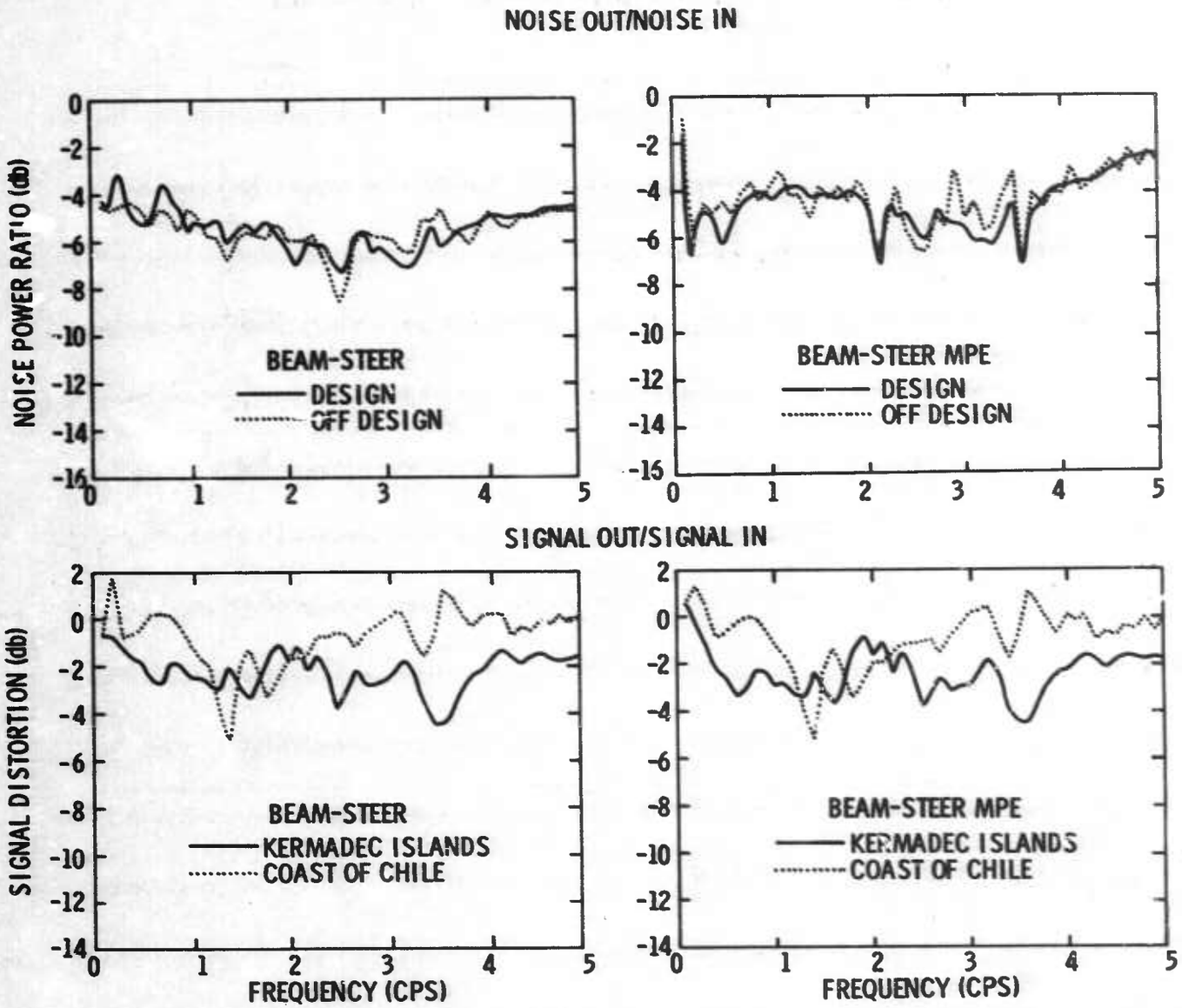

Figure V-9. Noise and Signal Ratios for Beam-Steer Processors

The results of applying the 9-channel MCF are shown in Figure V-10. Figure V-11 shows the corresponding noise and signal power ratios. The $\sqrt{n}$ (10 db) noise rejection obtained by the filter over the usable seismic band was exceeded slightly (11 db) overall with 13 db achieved in the partly correlated 4- to 6-sec microseism band. The filter caused a signal distortion of approximately 3 db for the Kermadec Islands signal and 2 db for the Chilean signal. The signal distortion exceeds that indicated by the amplitude response of the filter and is probably due to contamination of the transient signal by ambient noise, misalignment of the P-wave onsets and slight inequalization residuals.

In summary, the signal enhancement processors performed satisfactorily for rejection of uncorrelated noise in the frequency range from 0.3 to 1.3 cps, both in and outside of the design interval. Both the beam-steer of the MPE outputs and the 9-channel MCF filters attained noise rejection slightly greater than the $\sqrt{n}$ in the 0.1 to 0.3 cps frequency band where some correlated microseism energy exists. A comparison of the various signal enhancement processor outputs is presented in Figure V-12.

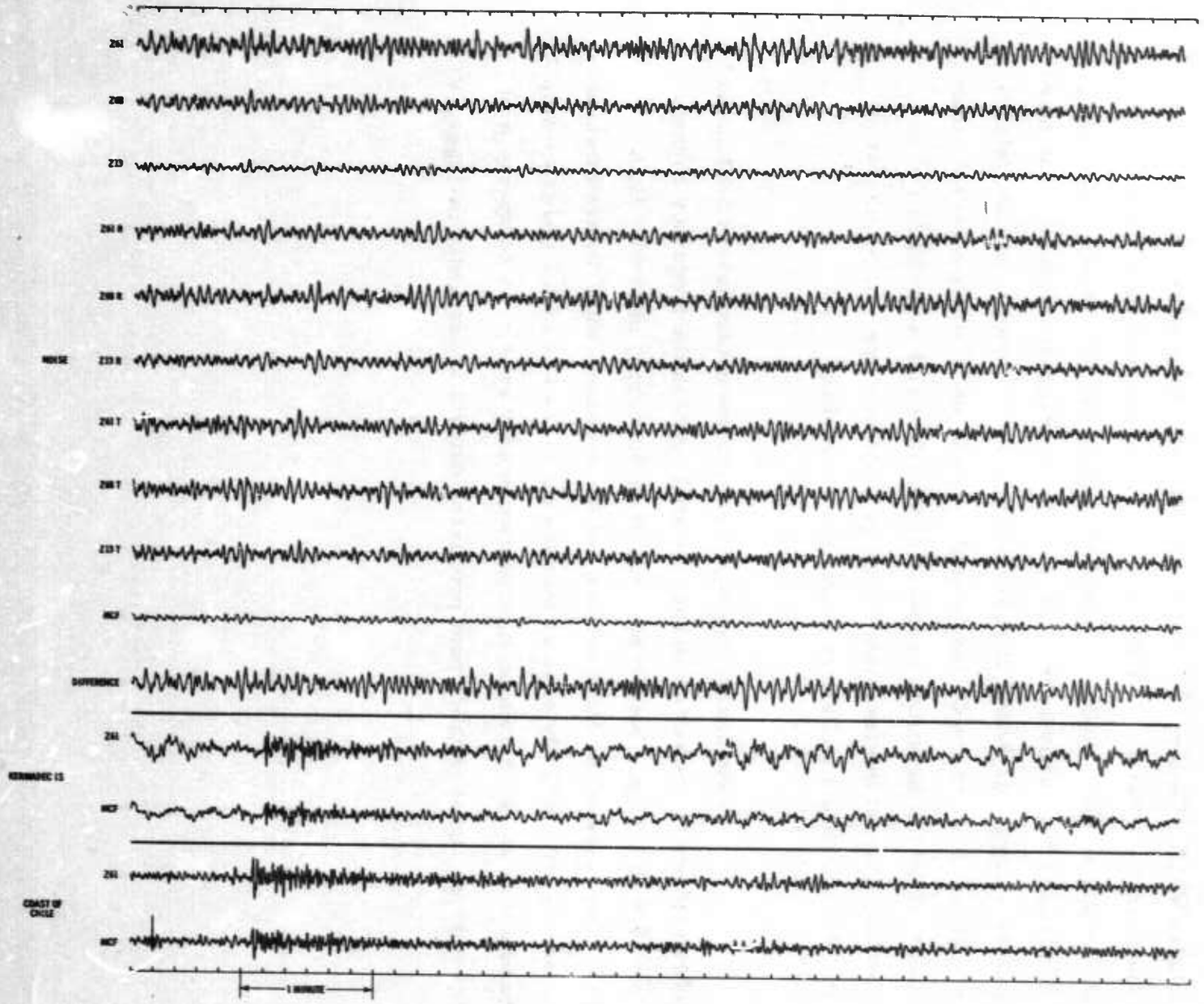

Figure V-10. Results of Applying 9-Channel Signal Extraction Processor

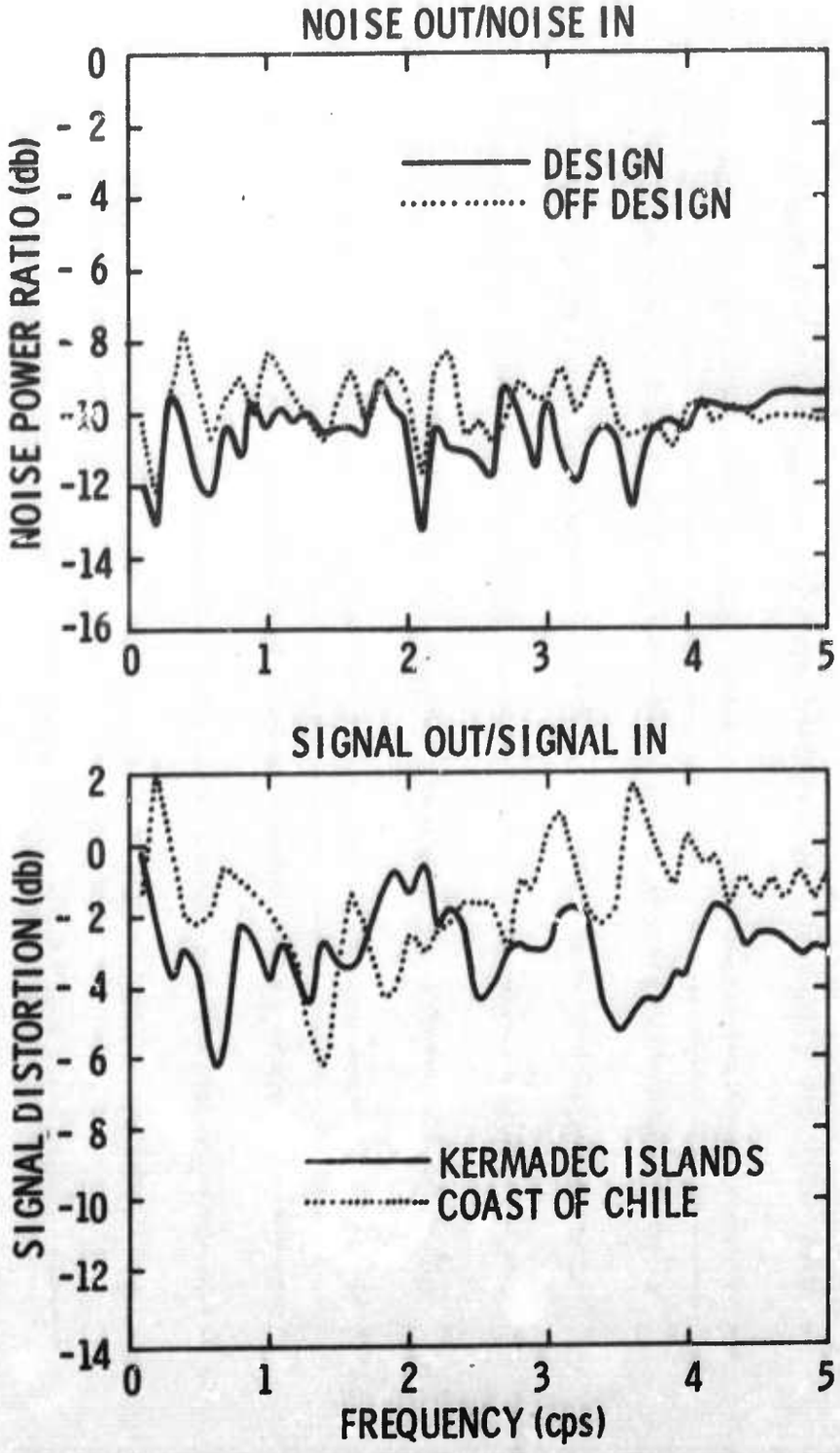

Figure V-11. Noise and Signal Ratios for 9-Channel Signal Extraction Processors

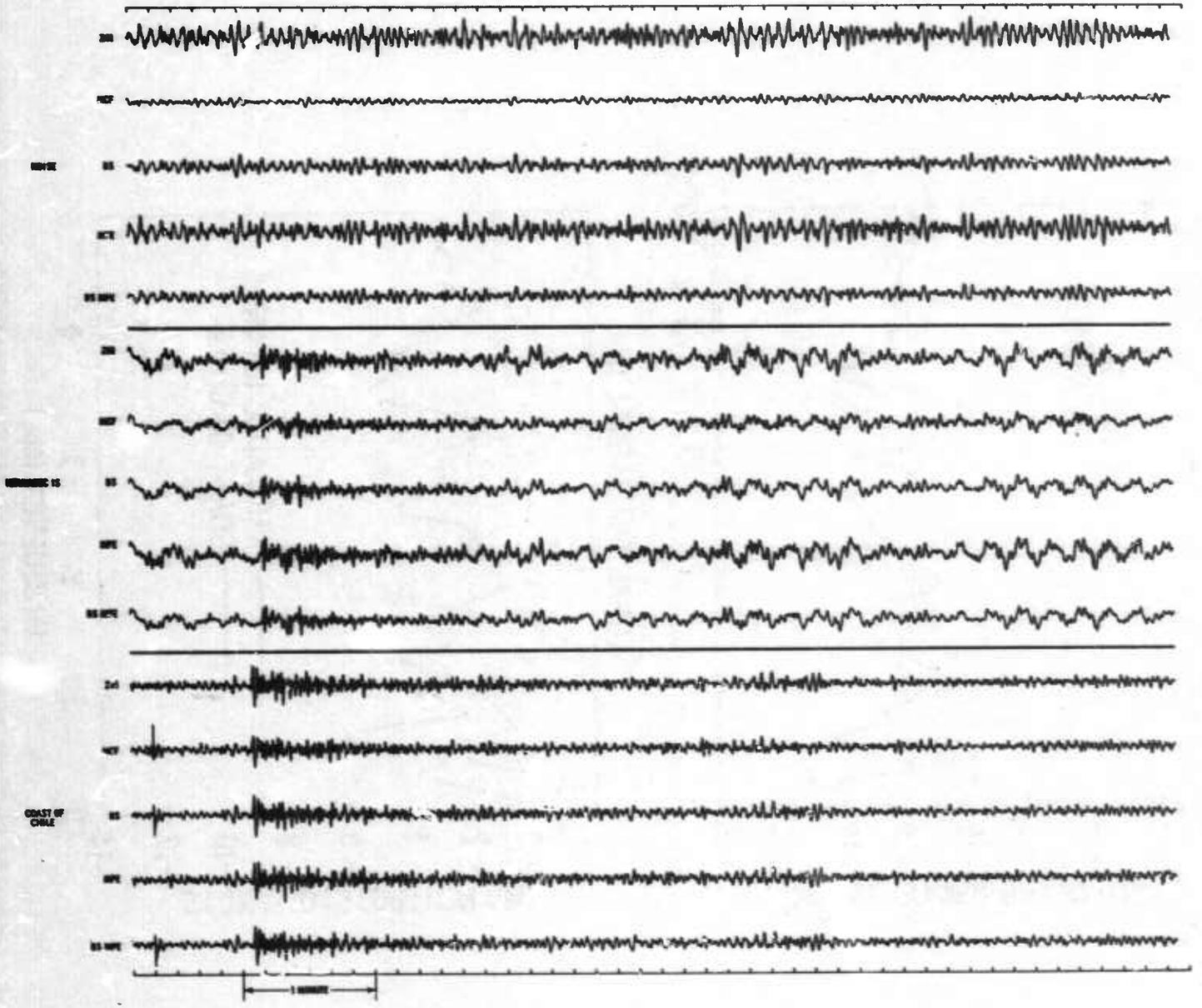

Figure V-12. Comparison of Short-Period Signal Enhancement Processors

SECTION VI
CONCLUSIONS

The use of 3-component instrumentation provides a capability for noise rejection by exploiting the relationship between horizontal and vertical components of the seismic noise field. For extended arrays in general and TFO in particular, it is possible for local geological and topological features to disturb the propagation of low-velocity surface wave energy across the array, causing a less coherent noise component which cannot be as effectively removed by array velocity filtering. However, at each instrument location, a portion of the vertical component of the surface wave energy can be interpolated from horizontal instruments and then removed from the vertical recording. The objective of the analysis was experimental verification of the effectiveness of such 3-component processors for teleseismic signal extraction.

Prior to the design of the signal enhancement processors, long-period and short-period teleseismic signal coherence and equalization were examined. These studies indicate extremely reproducible P-waves across the TFO array. In addition, the long-period S-phase energy appears well equalized, suggesting that crustal filtering variations across the array are small for vertically traveling energy. Similar analysis of long-period surface waves shows a more severe problem for horizontally traveling energy. Long-period spectral variations in the range of peak signal power are approximately ±1 db for P-waves, ±3 db for S-waves and ±6 db for surface waves. P- and S-waves yielded high coherences in the frequency band from 0.02 to 0.08 cps, while surface wave coherence was very small. The orientation of the horizontal components varied by as much as 15° which partly contributed to the observed surface wave inequalization. However, it is also

probable that surface waves cannot traverse the array undistrubed but undergo scattering that decreases the coherence. Short-period P-phase spectra yield ±2 db variation over the peak signal band, indicating that the vertical component magnification compensations (derived from on-site calibrations) were reasonably correct for these signals. Signal coherence is high over this band.

For the receiver separations used in the study, both the vertical and horizontal noise fields are essentially uncorrelated. Thus, vertical-component or horizontal-component array processors would not be expected to exceed the $\sqrt{n}$ improvement in rms signal-to-noise ratio possible from simple time-shifting-and-summing. Such is found to be the case for the 5-channel vertical MCF and the 9-channel MPE (long-period), except for an indicated noise directionality around 0.12 cps. The 5-channel case closely approximates the theoretical rejection level of 7 db. For the 9-channel MPE, the summing of eight uncorrelated horizontal components yields an output 9 db down in power from the vertical, thus the vertical noise level was virtually unaffected.

In general, the 3-channel MPE outputs and the 9-channel (tripartite) multichannel filters also achieved a $\sqrt{n}$ noise rejection over the usable seismic band. Some vertical-horizontal noise coherence was detected by the long-period processors at about 0.12 cps for an additional 3-db rejection and by the short-period processors from about 0.2 to 0.5 cps for 2 db additional noise rejection. These confirm the peaks in the predictability curves. While the magnitude of additional rejection is not great, it is important to recall that the noise field is essentially totally uncorrelated between like components across the array, and these gains would probably not be realized through conventional vertical array processing.

Processor performance were similar both in and adjacent to the noise design interval, suggesting that the process is reasonably time-stationary. Insufficient noise preceded the signal onsets to evaluate noise rejection for the signal samples. Averaged noise statistics would certainly be preferable for the design of long-term, time-invariant filters, but adaptive filtering should provide an attractive alternative to the compromise of averaging.

In summary, 3-component preprocessing appears to be feasible for rejection from the vertical recording of surface wave seismic noise and horizontally scattered signal energy and should be especially effective where local geology interferes with surface wave coherence across the array.

SECTION VII

REFERENCES

1. Texas Instruments Incorporated, 1965: Theoretical Capability of Systems of Horizontal Seismometers for Predicting a Vertical Component in Ambient Trapped-Mode Noise, Array Research Spec. Rpt. No. 7, Contract AF 33(657)-12747, 9 Nov.

2. Texas Instruments Incorporated, 1966: Data Collection Array Research Spec. Rpt. No. 12, Contract AF 33(657)-12747, 8 Apr.

3. Texas Instruments Incorporated, 1966: Initial Analysis of Long-Period Large-Aperture Data Recorded at the Tonto Forest Seismological Observatory in 1965, Array Research Spec. Rpt. No. 16, Contract AF 33(657)-12747, 31 Aug.

4. Texas Instruments Incorporated, 1966: Ambient Noise Analysis of 3-Component Short-Period Data Recorded at Tonto Forest Seismological Observatory, Array Research Spec. Rpt. No. 18, Contract AF 33(657)-12747, 15 Nov.

5. Texas Instruments Incorporated, 1965: Array Research Semiannual Tech. Rpt. No. 3, Section VI, Contract AF 33(657)-12747, 3 Jun.

6. Texas Instruments Incorporated, 1966: Array Research Semiannual Tech. Rpt. No. 5, Section VII, Contract AF 33(657)-12747, 1 Jul.

7. Texas Instruments Incorporated, 1966: Array Research Semiannual Tech. Rpt. No. 5, Section II, Contract AF 33(657)-12747, 1 Jul.